POSITION ESTIMATION FOR IR-UWB SYSTEMS USING COMPRESSIVE SENSING

A Degree Thesis

Submitted to the Faculty of the

Escola Tècnica d'Enginyeria de Telecomunicació de Barcelona

Universitat Politècnica de Catalunya

by

Ricardo García Gutiérrez

In partial fulfilment

Of the requirements for the degree in

TELECOMMUNICATIONS SYSTEMS ENGINEERING

Advisor: Montse Nájar Marton

Barcelona, June 2016

Abstract

Recently, a growing interest in precise indoor wireless locating systems has been observed. Indoor environments are typically complex wireless propagation channels with numerous multi-paths created by closely spaced scattering objects. The ability to resolve these multi-paths is very important for good ranging resolution and positioning accuracy. Impulse-Radio Ultra-Wideband (IR-UWB) is a promising technology to fulfill these requirements in harsh indoor propagation environments due to its great time resolution and immunity to multipath fading. One of the major IR-UWB signal processing challenges is the high sampling demands of IR-UWB digital receivers, which greatly elevates the cost and power consumption of IR-UWB systems . Compressive Sensing provides a solution by allowing them to sample IR-UWB signals at a lower rate than the Nyquist sampling limit.

The CS approach relies on the fact sparse representations are possible in the localization context. Basically two sparsity patterns can be exploited: Firstly, transmitting an ultra-short pulse through a multipath UWB channel leads to a received UWB signal that can be approximated by a linear combination of a few atoms from a pre-defined dictionary, yielding thus a sparse representation of the received UWB signal. Secondly, the inherent spatial sparsity of scene can be introduced through the use of an overcomplete basis or dictionary that enables to jointly evaluate all multiple location hypothesis.

In this degree thesis, three novel data-acquisition and positioning methods exploiting different sparse representations for IR-UWB signals under challenging indoor environments are presented. Essentially, through the formulation of sparsity-based reconstruction techniques it is viable to localize targets while reducing the computational load and sampling requirements. Their performance is assessed and compared under the framework of the IEE.802.15.14a channel models, which is a standard developed specifically for UWB wireless positioning.

Resum

Recentment, s'ha observat un interès creixent en els sistemes de localització passiva sense fil per a edificis interiors com oficines o naus industrials. Típicament, els ambients d'interiors són canals de propagació complexos amb nombroses reflexions creades per objectes dispersius molt pròxims entre si. La capacitat de resoldre aquests múltiples camins és molt important per a una bona resolució d'abast i precisió de posicionament. Impuls-ràdio de banda ultra-ampla (UWB-IR) és una tecnologia prometedora per complir amb aquests requisits en entorns de propagació interiors a causa de la seva gran resolució temporal i la immunitat al esvaniment per múltiples camins. Un dels principals reptes de processament de senyals IR-UWB és l'alta demanda de mostreig dels receptors digitals IR-UWB, el que eleva considerablement el cost i el consum d'energia dels sistemes IR-UWB. *Compressive Sensing* proporciona una solució en la qual permet mostrejar senyals IR-UWB a un ritme menor que el límit de mostreig proposat per Nyquist.

L'enfocament d'aquest problema amb *Compressive Sensing* es basa en el fet que representacions disperses són possibles en el context de la localització. Bàsicament dos patrons de dispersió poden ser explotats: En primer lloc, la transmissió d'un pols de molt poca duració a través d'un canal de banda ample on la senyal experimenta múltiples trajectes, això condueix a una senyal de *UltraWideband* rebuda que pot ser aproximada per una combinació lineal d'uns pocs àtoms d'un diccionari predefinit, obtenint-se així una representació dispersa. En segon lloc, l'escassetat de objectius a localitzar en l'escena es pot utilitzar mitjançant l'ús d'un diccionari sobre-complet que permeti avaluar conjuntament les múltiples hipòtesis d'ubicació en un escenari bidimensional, adquirint així una representació dispersa.

En aquest projecte final de carrera, es presenten tres nous mètodes d'adquisició de dades i posicionament que exploten diferents representacions disperses per senyals IR-UWB sota ambients interiors. En essència es planteja, mitjançant la formulació de tècniques de reconstrucció de *Compressive Sensing*, que és viable localitzar objectius i al mateix temps reduir els requisits de càrrega computacional i alts ritmes de mostreig. El rendiment dels algoritmes proposats s'avalua i es comparen en el marc dels models de canal IEE.802.15.14a, que és un estàndard desenvolupat específicament per al posicionament sense fil en sistemes *UltraWideband*.

Resumen

Recientemente, se ha observado un interés creciente en los sistemas de localización pasiva inalámbrica para edificios interiores como oficinas o naves industriales. Típicamente, los ambientes de interiores son canales de propagación inalámbricos complejos con numerosas reflexiones creadas por objetos dispersivos muy próximos entre sí. La capacidad de resolver estos múltiples caminos es muy importante para una buena resolución de alcance y precisión de posicionamiento. Impulso-radio de banda ultra-ancha (UWB-IR) es una tecnología prometedora para cumplir con estos requisitos en entornos de propagación interiores debido a su gran resolución temporal y la inmunidad al desvanecimiento por múltiples caminos. Uno de los principales retos de procesamiento de señales IR-UWB es la alta demanda de muestreo de receptores digitales IR-UWB, lo que eleva considerablemente el costo y el consumo de energía de los sistemas IR-UWB. *Compressive Sensing* proporciona una solución que permite muestrear señales IR-UWB a un ritmo menor que el límite de muestreo propuesto por Nyquist.

El enfoque de este problema con *Compressive Sensing* se basa en el hecho de que representaciones dispersas son posibles en el contexto de la localización. Básicamente dos patrones de dispersión pueden ser explotados: En primer lugar, la transmisión de un pulso ultra corto, través de un canal de banda ancha donde la señal experimenta trayectos múltiples, conduce a una señal de *UltraWideband* recibida que puede ser aproximada por una combinación lineal de unos pocos átomos de un diccionario predefinido, obteniéndose así una representación dispersa de la señal de UWB recibida. En segundo lugar, la escasez de objetivos a localizar de la escena se puede utilizar mediante el uso de un diccionario sobre-completo que permita evaluar conjuntamente las múltiples hipótesis de ubicación en un escenario bidimensional, adquiriendo así una representación dispersa, con pocos elementos.

En este proyecto final de carrera, se presentan tres nuevos métodos de adquisición de datos y posicionamiento que explotan diferentes representaciones dispersas para señales IR-UWB bajo ambientes interiores. En esencia se plantea, mediante la formulación de técnicas de reconstrucción de *Compressive Sensing*, que es viable localizar objetivos y al mismo tiempo reducir los requisitos de carga computacional y altos ritmos de muestreo. El rendimiento de los algoritmos propuestos se evalúa y se compara en el marco de los modelos de canal IEE.802.15.14a, que es un estándar desarrollado específicamente para el posicionamiento inalámbrico en sistemas *UltraWideband*.

Acknowledgements

First and foremost, I would like to thank to my thesis advisor, Prof. Montse Nájar, for being a helpful guide during my first steps in the world of research. I don't want to forget mentioning Genís, who has been my work colleague in this degree thesis. I am thankful for the great quality time spent on discussions with him about the project.

I am thankful to my colleagues at the UPC for all these years at the faculty and to my friends in Reus. Finally, thanks so much to my family for being a fundamental piece of this.

Revision history and approval record

Revision	Date	Purpose
0	10/06/2016	Document creation
1	27/06/2016	Document revision

DOCUMENT DISTRIBUTION LIST

Name	e-mail
Ricardo García Gutiérrez	riki_10004@hotmail.com
Montse Nájar Marton	montse.najar@upc.edu
Eva Lagunas Targar ona	eva.lagunas@uni.lu

Written by:		Reviewed and approved by:	
Date	26/06/2016	Date	dd/mm/yyyy
Name	Ricardo Garcia Gutiérrez	Name	Montse Nájar Marton
Position	Project Author	Position	Project Supervisor

Table of contents

List of Figures

List of Tables:

Glossary

ADC Analog-to-Digital Converter

AIC Analog-to-Information Converter

AWGN Additive White Gaussian Noise

ECC Electronic Communications Committee

CS Compressed Sensing

OMP Orthogonal Matching Pursuit

CoSaMP Compressive Sampling Matching Pursuit

DSP Digital Signal Processing

FCC Federal Communications Commission

FFT Fast Fourier Transform

IEEE Institute of Electronical and Electrics Engineers

i.i.d. Independent and Identically Distributed

LOS Line of Sight

LP Linear Program

LS Least Squares

ML Maximum Likelihood

MP Matching Pursuit

MPC MultiPath Components

TOA Time of Arrival

RIP Restricted Isometry Property

RMSE Root Mean Squared Error

SNR Signal to Noise Ratio

UWB Ultra WideBand

1. Introduction

1.1. Objective

The purpose of this project is to assess the problem of localization in IR-UWB systems using a Compressive Sensing. Impulse Radio Ultra-Wideband has emerged as a promising candidate for positioning passive nodes in wireless networks due to its fine time resolution that provides good ability to distinguish multipath components and great positioning capabilities. One major challenge in IR-UWB signal processing is the requirement of high sampling rate which leads to prohibitive cost of signal acquisition and a high computational load for the positioning estimation process. By exploiting different kinds of sparsity's patterns using CS based techniques, these requirements can be greatly relaxed without compromising the estimation accuracy provided by traditional sampling schemes.

The project main goals are:

- Apply CS-based techniques to solve the localization problem by exploiting the inherent sparseness structure of the context of the problem.
- Assure the estimation accuracy in multipath conditions and in the reduction of amount of data processed introduced by CS.
- Survey the literature of CS recovery algorithms and model the ones fitted to the problem's environment.
- Analyze the performance of CS reconstruction methods combined with the problem's model proposed.

1.2. Requirements & Specifications

Project requirements:

- Extended analysis of the Compressive Sensing theory applied to the positioning problem in IR-UWB systems
- Validation of the performance and feasibility by numerical assessment of the CS-Positioning techniques in rich multipath propagation conditions produced by the challenging environments.
- Acceptable estimation accuracy
- Significate reduction of computational complexity and load.

Project specifications:

- Target environment: Mostly indoor and outdoor suburban-like environments of small to medium ranges, alternating models with NLOS /LOS paths.
- Channel model: Modified Saleh-Valenzuela model proposed for the IEE 802.15.4a physical layer with frequency ranges of 2 GHz – 10 GHz (UWB) whose parameters vary with environments above.
- Number of potential targets: 1
- Number of anchor nodes: 4
- IR-UWB system model: The transmitting device is assumed to transmit periodic frames of Gaussian pulses of very short duration.

- Greedy sparsity recovery algorithms:
    - Matching Pursuit techniques and its extended version : Orthogonal Matching Pursuit (OMP)
    - Compressive Sampling Matching Pursuit (CoSaMP)
    - Model-based compressive sampling

1.3. Methods

This project is basically the continuation of the supervisor's previous work in the field of Position Estimation using ultra-wideband signals, the main ideas behind it as well. This work is developed in the framework of the Department of Signal Theory and Communications.

1.4. Work plan

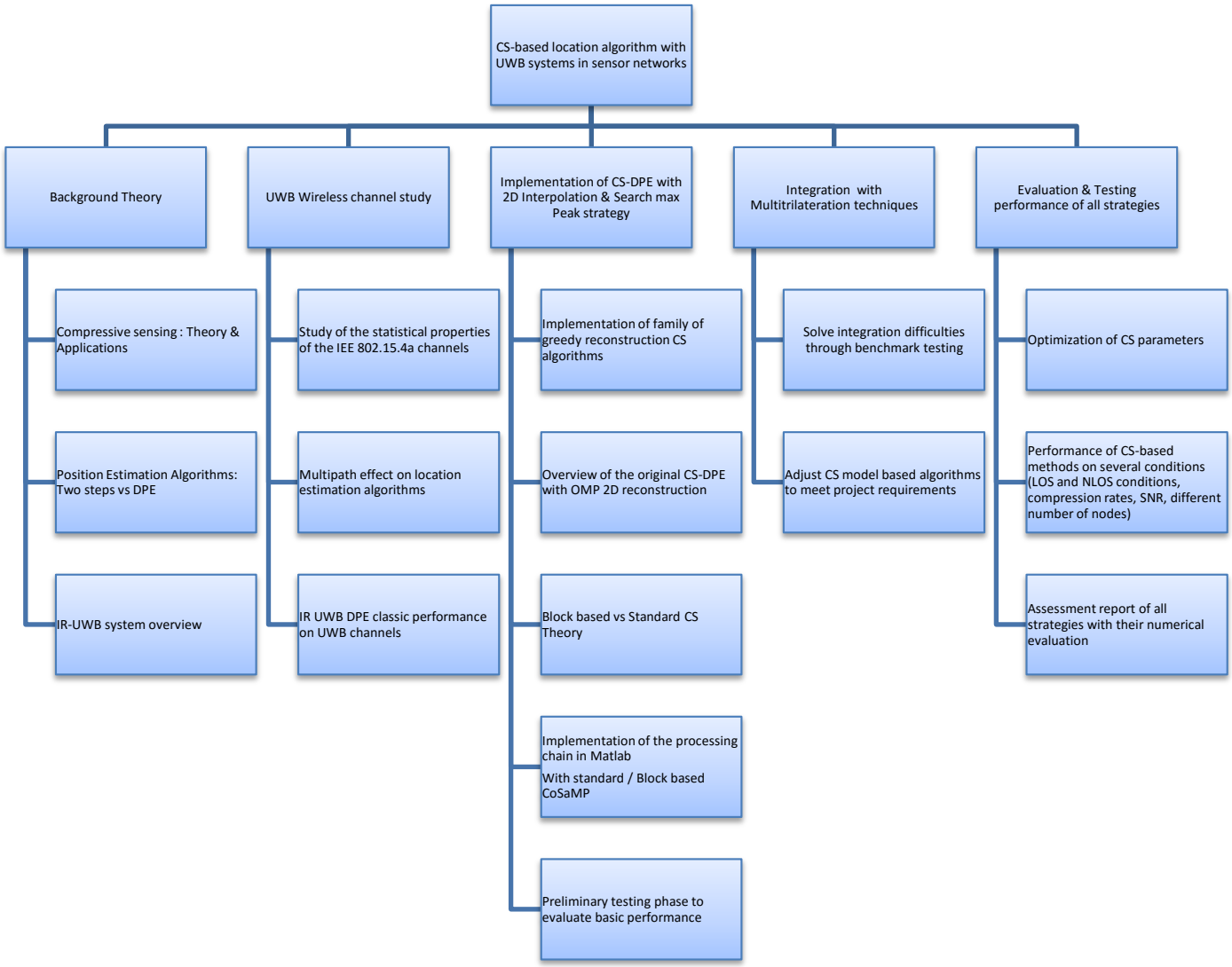
CS-based location algorithm with UWB systems in sensor networks
Background Theory
UWB Wireless channel study
Implementation of CS-DPE with 2D Interpolation & Search max Peak strategy
Integration with Multitrilateration techniques
Evaluation & Testing performance of all strategies
Compressive sensing : Theory & Applications
Position Estimation Algorithms: Two steps vs DPE
IR-UWB system overview
Study of the statistical properties of the IEE 802.15.4a channels
Multipath effect on location estimation algorithms
IR UWB DPE classic performance on UWB channels
Implementation of family of greedy reconstruction CS algorithms
Overview of the original CS-DPE with OMP 2D reconstruction
Block based vs Standard CS Theory
Implementation of the processing chain in Matlab
With standard / Block based CoSaMP
Preliminary testing phase to evaluate basic performance
Solve integration difficulties through benchmark testing
Adjust CS model based algorithms to meet project requirements
Optimization of CS parameters
Performance of CS-based methods on several conditions (LOS and NLOS conditions, compression rates, SNR, different number of nodes)
Assessment report of all strategies with their numerical evaluation

2. State of the art of the technology used or applied in this thesis:

A background, comprehensive review of the literature is required. This is known as the Review of Literature and should include relevant, recent research that has been done on the subject matter.

2.1. Compressive sensing

Conventional approaches to sampling signals or images follow Shannon's theorem: the sampling rate must be at least twice the maximum frequency in the signal (the so-called Nyquist rate). CS establishes a novel sensing / sampling paradigm by suggesting it may be possible to surpass the traditional limits of sampling theory.

The field of CS grew out of the work of *Candès*, *Romberg*, *Tao* and *Donoho*, who showed that a finite-dimensional signal having a sparse or compressible representation can be recovered from a small set of linear, non-adaptive measurements [1, 2, 3, 4].

The amount of data generated by sensing systems has grown from a trickle to a torrent. Unfortunately, in many important and emerging applications, the resulting Nyquist rate is so high that we end up with far too many samples. Alternatively, it may simply too costly, or even physical impossible, to build devices capable of acquiring samples at the necessary rate.

CS theory builds upon the fundamental fact that we can represent many signals using only a few non-zero coefficients (sparse representation) in suitable basis or dictionary.

Nonlinear optimization can then enable recovery of such signals from fewer measurements than traditional methods. Rather than first sampling at a high rate and then compress the sampled data, CS finds a way to directly sense the data in a compressed form.

In communications systems such as Ultra-Wideband (UWB), where the Analog-to-digital (ADC) converters are a major challenge in practical implementations, CS emerges as a robust alternative to address the issue.

2.1.1. Review of Compressive Sensing

This section presents briefly the main ideas behind compressive sensing and its mathematical foundations.

Consider a real-valued, finite length, discrete time signal $x \in \mathbb{R}^M$ which can be expressed in orthonormal basis $\psi = [\psi_1 \psi_2 \dots \psi_M]$ as follows:

$$x = \sum_{i=1}^{M} \psi_i \theta_i \qquad (2.1)$$

Where the vector $\theta = [\theta_1 \dots \theta_M]$ is the sparse vector, whose coefficients are mostly zero.

It can also be represented by matrix notation:

$$x = \Psi\theta \tag{2.2}$$

The matrix Ψ , the dictionary where θ becomes sparse, has dimensions MxM.

2.1.2. Sparsity

Many natural signals have concise representations when expressed in a convenient basis. Consider, for example, an image and its wavelet transform. Although nearly all the image pixels have nonzero values, the wavelet coefficients offer a concise summary: most coefficients are small, and the relatively few large coefficients capture most of the information.

So the implication of sparsity seems now clear: when a signal has a sparse representation, one can discard the small coefficients without too much perceptual loss. This is the principle used in many modern lossy coders such as JPEG.

Mathematically, we say that a signal θ is K-sparse when it has at most K << M non-zeros:

$$\|\theta\|_0 \leq K.\ We\ let\ \Sigma k = \{\theta : \|\theta\|_0 \leq K\}. \tag{2.3}$$

Typically, signals are not truly sparse, but admit a more or less sparse representation in some basis Ψ. These set of signals are called compressible in the sense that the magnitude of their coefficients, when sorted, decay rapidly.

The assumption of sparsity, along with the compressibility, is a requirement in order for the reconstruction process to succeed.

2.1.3. Measurement or sensing matrix

As mentioned earlier, when CS theory is applied to communications, the sampling rate can be reduced. How this is exactly achieved? First of all, consider the classical linear measurement model for the above signal:

$$y = \Phi x = \Phi\Psi\theta \tag{2.4}$$

Where Φ is the measurement matrix, whose dimensions are NxM $(N < M)$.This matrix projects the signal x into a lower dimensional space and forms the measurements vector y.The construction of sensing schemes is a central challenge in the area of CS research from both the practical and theoretical point of view. The difficulties arise in the practical situations or real systems, constructing new frameworks in Analog-to-information conversion (AIC) as an alternative to traditional ADC is not as clear as the matrix notation stated above. This thesis does not study the feasibility of these hardware implementations.

But how is this measurement matrix designed?

Instead of describing a design procedure, we will focus on a number of desirable properties that these matrices must satisfy, which are listed below.

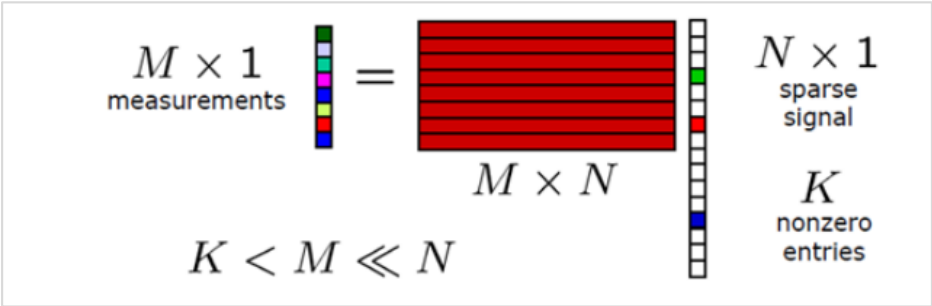

FIGURE 2.1: Compressive Sensing Matrix equation

2.1.4. Properties of the sensing matrices

2.1.4.1. Null space conditions

A natural place to begin is by considering the null space of Φ, denoted $N(\Phi) = \{z : \Phi z = 0\}$. If we wish to be able to recover all sparse signals θ from the measurements y, then it is immediately clear that for any pair of distinct vectors $\theta, \theta' \in \Sigma k$, we must have $\Phi x \neq \Phi x'$, since otherwise it would be impossible to distinguish x from x' based solely on the measurements y

2.1.4.2. Mutual Coherence

Another concept that plays an important role on the guarantees of better CS is coherence.

The coherence is defined as the maximum value amongst inner product of the orthonormal representation basis and the orthonormal measurement matrix. A low value is desirable in order to ensure mutually independent matrices. The coherence can be measured:

$$\mu(\Phi, \Psi) = \max \left|\langle \phi_k, \psi_j \rangle\right| \quad 1 \leq k \leq N \,, 1 \leq j \leq M \tag{2.5}$$

Verifying that a matrix obeys this property is computationally feasible, unlike the other properties. Hence, its importance to provide concrete recovery guarantees.

2.1.4.3. Restricted Isometry Property

In [5], Candès and Tao introduced the following isometry condition on matrices Φ and established its important role in CS. This is also the most widely used criterion for evaluating the quality of a CS measurement matrix. It can be summarized as follows:

Definition 1. *A matrix A satisfies the restricted isometry property (RIP) of order k if there exists a $\delta k \in (0,1)$ such that $(1 - \delta k)\ \|\theta\|_2^2 \leq \|\Phi\Psi\theta\|_2^2 \leq (1 + \delta k)$ holds for all $\theta \in \Sigma k$.*

The important question is how can one create a matrix Φ, given the basis Ψ, so that Φ has the RIP of high order? Verifying that any given matrix has this property is computationally intensive and involves checking all $\binom{n}{k}$ submatrices with k columns of $\Phi\Psi$. One approach to obtain a matrix Φ with the RIP of high order is to use random matrices. The $N \times M$ matrices can be generated according to the following rules:

- Form Φ by sampling N column vectors uniformly on the unit sphere in $\mathbb{R}^M$.

- Let the entries of Φ be *i.i.d.* normal with zero mean and unit variance.

All obey the restricted isometry property of order k provided that $N > C \cdot K \log(M/K)$, for some constant C, therefore establishing a lower bound on the measurements needed. These matrices also are highly incoherent with any fixed basis with high probability as well. Thus, random projections plays a central role as a universal measurement basis.

Not all of these conditions are necessary, but for stable recovery and robustness against noise, it is indispensable to satisfy them.

2.1.5. Signal Reconstruction Algorithms

Since N << M, the system has more unknowns than equations, and thus the system is not invertible .There are variety of methods that are able to solve the optimization problem.

Since the l_2 norm or least squares minimisation does not usually return a sparse vector, alternatives have been sought. One way is to directly force a constraint sparsity, using the l_0 norm, but solving this minimisation program is an NP-complete problem, in other words, is computational intensive. Although it gives the correct results, the strategy becomes too costly and inefficient.

Since, out of the infinite solutions to the system, the CS interest lies in recovering the sparsest solution, l_1 minimisation comes as a firm candidate.

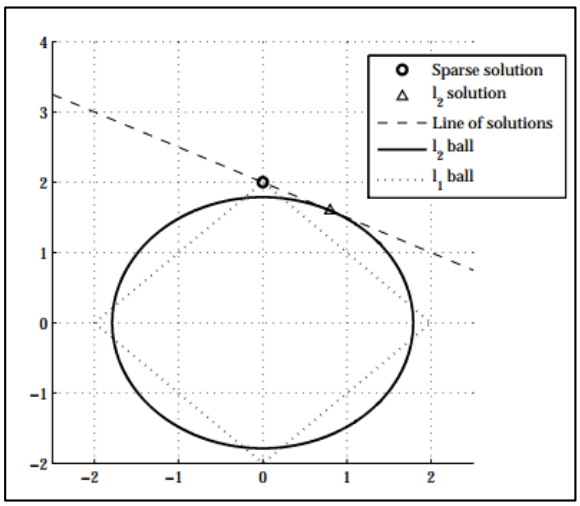

FIGURE 2.2: Solving the l_1 and l_2 minimisation problem in $\mathbb{R}^2$.The dotted line represents the sparse solutions. The sparsest solution comes with $l_1$minimisation.

This procedure can be re-written as a convex optimization task and, also reinterpreted as a linear program.

It is shown in [6] that the following linear program can exactly reconstruct the signal with high probability, if the RIP property holds, the vector is sufficiently sparse and the number of measurements is above the mentioned bound:

$$\min_{\theta \in \mathbb{R}^M} \|\theta\|_{l1} \; subject\ to \; y = \Phi\Psi\theta \tag{2.6}$$

Now, this belongs to the noise-free case, in real systems, measurements are noisy and the reconstruction program is reformulated, but it still can be solved with convex relaxed optimisation techniques:

$$\min_{\theta \in \mathbb{R}^M} \|\theta\|_{l1} \; subject\ to \; \|y - \Phi\Psi\theta\|_{l2} \leq \epsilon \tag{2.7}$$

In the literature, there are two great families of solvers for (2.7) that are used in the field of CS. One of them is the already stated *Convex Relaxation or* l_1 *minimisation* algorithms, based on linear programming techniques such as BS (Basis Pursuit), but these often become too intractable when working with large scale problems. The other alternative is *Greedy Pursuit* algorithms, who belong to a class sub-optimal iterative solvers that are very popular in the sparse signal reconstruction field.

2.1.6. Greedy Pursuit Algorithms

Greedy pursuit is a class of nonlinear iterative algorithms, that are also called *Matching Pursuit*, where at each step, atoms (columns of the $\boldsymbol{\Phi\Psi}$) are selected in a greedy fashion to best approximate the signal. The matching procedures present polynomial running times and are more computationally efficient than most convex $\boldsymbol{l_1}$ optimization techniques. In the following sub-section I present a few of the most popular variants:

2.1.6.1. Orthogonal Matching Pursuit (OMP)

OMP is a simple and improved variant of matching pursuit algorithms. Its operation is based on the principle mentioned above and goes as follows: Firstly, selects the atom of the dictionary ($\Phi\Psi$) most correlated at each step, then it projects the signal orthogonally onto the subspace spanned by the candidate atoms, by adopting a least squares step, and finally it updates the residual.

The improvement lies on the fact that the algorithm does not pick twice the same atom thanks to the orthogonality introduced in the residual, even though it comes with the expense of more computation.

OMP has a few more drawbacks such as poor robustness against noise, unknown success when the signal is compressible, non-uniform guarantees of success as l_1 convex minimization and, finally, the requirement of the level of sparsity. Therefore, the performance of OMP can be weak if its settings are not chosen right.

2.1.6.2. Compressive Sampling Matching Pursuit (CoSaMP)

An extension to orthogonal matching pursuit algorithms is the CoSaMP (*COmpressive SAmpling Matching Pursuit*) algorithm published in [7] .CoSaMP serves as an improved version of OMP, since its time complexity is slightly better and assures more guarantees in terms of stability and uniformity as best optimization based approaches [7, 8]. The next summarized list details the basic steps behind the overall greedy iterative structure:

- **Identification**: Finds the largest 2K components of the signal proxy.
- **Support Merge**: Merges the support of the signal proxy with the support of the solution from the previous iteration.
- **Estimation**: Estimates a solution via least squares with the constraint that the solution lies on a particular support.
- **Pruning**: Takes the solution estimate and compresses it to the required support,
- **Sample Update**: Updates the "sample", namely the residual in $\Phi\Psi$ -space.

The performance of CoSaMP is compared with OMP, in terms of behavioural aspects like stability, running time and optimal number of samples, at this table:

	OMP	**CoSaMP**	**Convex Opt**
Sampling Matrix	Sub-Gaussian	Partially satisfy RIP	RIP
Opt. # Samples	Yes	Yes	Yes
Uniformity	No	Yes	Yes
Stability	? (Not Proven)	Yes	Yes
Running Time	$O(MN)$	$O(KMN)$	$LP(MN)$

TABLE 2.1: Comparison of CS algorithm's performances. M stands for # measurements, N for signal length and K refers to the sparsity level. LP (·) is the cost of a linear program

2.1.7. Model-Based Compressive Sensing

Standard CS dictates that robust signal recovery is possible from $N = O(K \cdot log\left(\frac{M}{K}\right))$ measurements. It is possible to substantially decrease the N bound by using more realistic signals models that go beyond the concept of simple sparsity [26].

These models correspond to a new class of structured compressible signals, whose coefficients are no longer strictly sparse but have a structured power-law decay, in other words, the assumption of the location of the non-zero components are no longer distributed randomly along the signal.

By reducing the number of degrees of freedom of a sparse / compressible signal by permitting only certain configurations of the large and zero/small coefficients, structured

sparsity models provide two immediate benefits to CS. First, they enable us to reduce, in some cases significantly, the number of measurements N required for stable recovery. Second, during signal recovery, they enable us to better differentiate true signal information from recovery artefacts, which leads to a more robust recovery.

UWB channels are modelled as sparse channels in which the delay spread can be very large due to the high dimensional signal space generated by their large bandwidth, but the number of significant paths is normally small, furthermore experimental studies have shown that the multipath arrives in a few clusters. A structured sparsity model exists for these kinds signal and is the so-called *Block sparsity model*.

The *Block sparsity* model consists of a class of signal vectors $x \in \mathbb{R}^{WJ}$, with W standing for the block length and J being the total number of blocks. This signal can be reshaped into WxJ matrix as follows:

$$\boldsymbol{X} = [\boldsymbol{x_1} \cdots \boldsymbol{x_J}] \in \mathbb{R}^{WxJ} \qquad (2.8)$$

The locations of the significant coefficients cluster in blocks under a specific sorting order. Typically examples, besides the one mentioned above, are DNA microarrays and magnetoencephalography, sensor networks and MIMO communications. In the last two cases, several signals share a common coefficient support, which can be exploited if the signals are concatenated, therefore exhibiting *Block sparsity*.

To incorporate this notion of block-structured sparsity into greedy recovery algorithms, a simple algorithm is constructed to obtain the best block-based approximation of the signal $\boldsymbol{X}$.

$$S(X, C) = \begin{cases} \boldsymbol{x_j} & \|\boldsymbol{x_j}\|^2 \geq \rho, \\ 0 & \|\boldsymbol{x_j}\|^2 < \rho, \end{cases} \qquad 1 \leq j \leq J \qquad (2.9)$$

Where C stands for the number of active clusters present on the signal. The approximation algorithm simply performs a column-wise hard thresholding. Let ρ be the C-th largest l_2 norm among the columns of $\boldsymbol{X}$. This framework can be extended to a block-compressible model where the l_2 norm of the blocks flows a power-law decay rate. It is noticeable that the level of sparsity is now $C \cdot W$.

In [26], significant improvements were shown. The block-based outperformed the traditional CoSaMP in running time because it involved sorting fewer coefficients in the approximation step and it required fewer iterations to converge. They also provided a theoretical framework for stable recovery for noisy measurements and block compressible signals. Finally, the lower bound of measurements needed for stable recovery was shown to be linear with sparsity, precisely, $N = O(CW)$.

A Block-based CoSaMP is developed in [26]. For more details of the algorithm implementation, please see the Appendix. There are other cluster-based greedy recovery algorithms [22], they can be classified based on the requirements of prior knowledge such as number of active clusters, size of clusters, the assumption of the locations of clusters in the signal space and the total level of sparsity .The following table summarizes them:

Algorithms	Num. of Clusters	Size of Clusters	Fixed Cluster Positions	Sparsity
Block CoSaMP	Yes	Yes	Yes	Yes
Block-CoSaMP with Dynamical Programming	Yes	No	No	Yes
Block OMP	Yes	Yes	Yes	Yes
CluSS MCMC	No	No	No	No

TABLE 2.2: Different Block-Based CS Algorithms

The *CluSS MCMC* algorithm [23] is based on a Bayesian approach to the Compressive Sensing cluster-based reconstruction procedure. It is very appealing since it does not require any prior knowledge of any kind, but for large scale applications it needs to perform a lot computation of hyper parameters. Block OMP [24] is a block sparse of the Orthogonal Matching Pursuit algorithm, whose performance is really similar to the Block-CoSaMP. The Block CoSaMP, with a dynamical programming approximation algorithm approach [25], eliminates the need for block sizes and it does not fix their positions in the signal space.

2.1.8. CS algorithms Stopping Criteria

The greedy CS reconstruction algorithms have an iterative nature, therefore a stopping criteria is needed for the algorithms to decide when to halt. One of the most widely used criteria is based on a heuristic metric, the residual of the approximation, when it drops a certain level the iteration process stops. But this would require knowledge of the noise magnitude or SNR at the receiver side, which would certainly not be realistic.

It is non-intuitive to decide which stopping criteria is the best, it mainly depends on the practical application and other factors. But for this thesis, a couple of natural methods will be used to stop the algorithms:

- A fixed number of iterations, set high enough to assure convergence.
- Difference between successive residual drops a certain tolerance.

Nonetheless, the OMP algorithm iterates a fixed number of times equal to the level of sparsity selected.

2.2. UWB Technology

In this section, the main characteristics of Ultra-Wideband (UWB) technology are discussed.

2.2.1. IR-UWB Overview

Ultra-wideband is a radio technology that can use a very low energy level for short-range, high-bandwidth communications over a large portion of the radio spectrum. The definition of UWB signals is related to the occupied frequency bandwidth. To specifically define what is meant by an UWB signal, the following fractional bandwidth definition is employed:

$$Bf = 2\frac{f_h - f_l}{f_h + f_l}$$

Where f_l and f_h are the lower and upper end (3 dB points) of the signal spectrum, respectively. UWB signals are then those signals that have a fractional bandwidth greater than $25\ \%$. On the other hand, according to the Federal Communications Commission (FCC) [9], a UWB signal is defined to have an absolute bandwidth of at least 500 MHz.

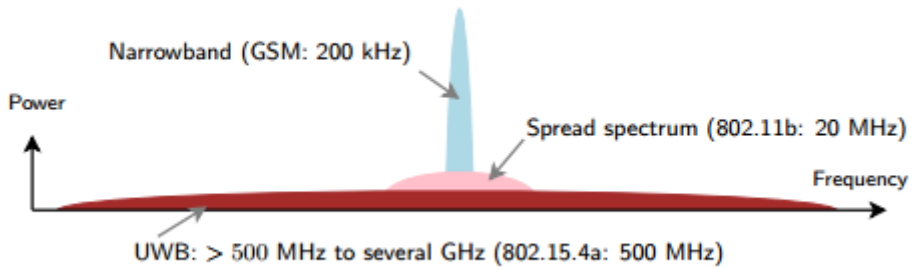

FIGURE 2.3: PSD (Power Spectral Density) of different RF signals

Specifically, Impulse radio UWB communicates with baseband pulses of very short duration, typically on the order of a nanosecond, thereby spreading the energy of the radio signal very thinly between DC and a few gigahertz.

The UWB is seen as the most serious candidate to achieve this vision of wireless interconnection between computing devices. Today, UWB is only at the beginning of its development for the consumer market. There is still a lot to be done to make this technology attractive. Other works around the standardization and the regulation are to be done, as well, in order to make UWB widespread and popular.

2.2.2. Characteristics and Challenges of IR-UWB systems

What makes UWB technology unique is that it has many attractive features for a high number of applications such as communications, sensors, positioning, tracking and radar.

IR-UWB radios can be designed with relatively low-complexity and low power consumption. The transmitter complexity can be greatly reduced, but the receiver side is

not exempt of design challenges such as high bandwidth A/D converters, Wideband LNA (Low-Noise Amplifiers) and low Signal to Noise ratio (SNR). The ultra-fine time resolution of these signals also require accurate timing source to keep up synchronisation.

Actually, the battery life in a UWB system will no longer be limited by the necessary emitted output power at the antenna, but by the backend consumption (modem and processing), which is prone to further enhancement with silicon downscaling and pulse detection techniques.

They are very suited in energy constrained, short-range wireless applications including personal-area-networks, low-power sensor networks, and wireless body-area-networks. Because of the bandwidths that can be achieved with IR-UWB radios, they are also used in precise location systems and for dedicated high-data-rate communication links.

The lack of available spectrum to support the growing number of wireless devices is well known. In the short-range application space, UWB can drive potential solutions for many of today's problems identified in the areas of spectrum management. The power spectral density (PSD) of UWB signals is extremely low, which enables UWB system to operate in the same spectrum with narrowband technology without causing undue interference.

2.2.3. UWB location systems

In the coming years, we will see the emergence of high-definition situation aware (HDSA) applications with capability to operate in harsh propagation environments where GPS typically fails, such as inside buildings. Such applications require localization systems with sub-meter accuracy.

Among the variety of prospective applications of IR-UWB, one of the most promising is in wireless sensor networks (WSNs), which require both robust communications and high-precision ranging capabilities.

Some of the reasons why UWB radio is considered a viable solution for precise localization systems are the great time resolution of the signal, which translates into good ranging accuracy, good ability to distinguish different arriving multi-path components (MPCs), robustness to multipath fading and penetrate obstacles. Proof of this was the introduction of an IR-UWB physical layer in the IEE 802.15.4a [10], a standard for low data rate communications combined with positioning capabilities.

Since IR-UWB signals have very short duration pulses, they can provide very accurate ranging and positioning capability in short range indoor radio propagation environments. Besides, the high time resolution characteristic of the UWB signal makes the time of arrival (TOA) method a good choice for location estimation in UWB communications.

2.3. Position Estimation Techniques

Recently, the subject of positioning in wireless networks has drawn considerable attention. With accurate position estimation, a variety of applications and services such as enhanced, improved fraud detection, location sensitive billing, intelligent transport systems and improved traffic management can become feasible for cellular networks .For short-range networks, on the other hand, position estimation facilitates applications such

as inventory tracking, intruder detection, tracking of fire-fighters and miners, home automation and patient monitoring

In order to realize potential applications of wireless positioning, accurate estimation of position should be performed even in challenging environments with multipath and non-line-of-sight (NLOS) propagation.

The localization approaches can be classified as self-positioning, where the target locates itself, and remote-positioning, where a central unit, with the help of information collected by reference nodes, estimates the target's position.

Impulse Radio Ultra-Wideband (IR-UWB) has emerged as a promising candidate for remote-positioning in wireless networks in challenging environments.

2.3.1. Two Steps vs. DPE schemes

Remote-positioning can also be further divided into two different estimation schemes. Direct positioning (DPE) refers to the case in which the position estimation is performed directly from the signals travelling between the nodes, the idea was firstly introduced by *Weiss* for narrowband systems in [11]. On the other hand, two-step positioning firstly extracts certain signal parameters, such as Angle of Arrival (AOA), Received Signal Strength (RSS) and Time of Arrival (TOA).Then estimates the position based on those signal parameters through the use of mapping (fingerprinting), geometric and statistical techniques.

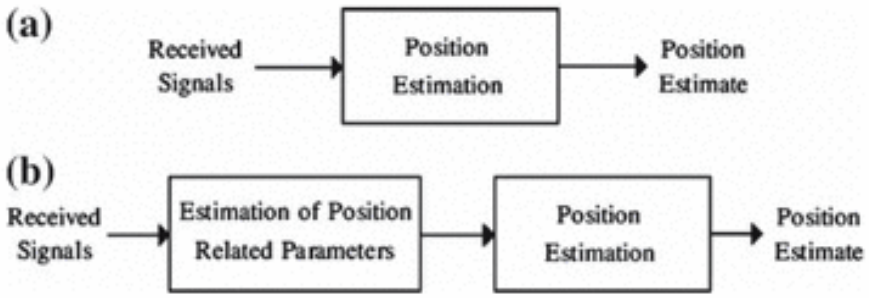

FIGURE 2.4: (a) DPE scheme (b) Two-steps scheme

There is quite interest in ranging-based algorithms in UWB-localization, especially the TOA algorithm, because they are very suited for these kind of systems due to their great time resolution.

The ToA (Time of Arrival) approach subdivides the problem: firstly, the ranging information between the target and the reference nodes is extracted, a simple trilateration or multi-trilateration, typically solved by least squares method, yields the location of the target node.

There are multiple versions of the ToA estimation phase based on their complexity and optimality such as the matched filter approach, which works by selecting the first peak after a given threshold of the correlation of the transmitted undistorted pulse with the received signal, and the non-coherent energy detectors, of less complexity because of their lower sampling requirements.

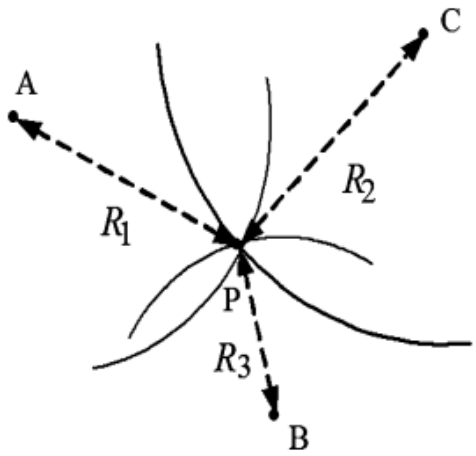

FIGURE 2.5: TOA Trilateration with three nodes

Nonetheless, the performance of two-steps can degrade significantly in low SNR and dense multipath conditions. However, recent work claim that this approach to positioning could be potentially improved, especially in challenging scenarios, if one treats the problem as a whole. That is to convert the two-step approach into a single-step procedure where digitized signals are combined to solve directly for the position coordinates. This positioning approach is known as Direct Position Estimation (DPE) in the literature. However, this comes with an increased computational complexity because the problem is now a single-multivariate non-convex optimization.

DPE also has the inconvenient of having to transmit the received signal of each reference node to a central processing unit, whereas two steps only requires the transmission of parameters. In IR-UWB localization systems, this could be a major challenge because massive amount of data are generated due to the high sampling needed for such large bandwidth.

Furthermore, the DPE procedure does not require a threshold selection, unlike many two steps approaches such as TOA where it can be a critical factor on performance accuracy.

DPE approaches have also been studied in GNSS systems, where in [12] was proven analytically to outperform two-steps procedures. In UWB systems, to name a few works, a MUSIC-algorithm type is proposed in [13], a frequency domain approach is submitted in [14] and a MLE (Maximum Likelihood Estimator) is introduced in [15].

2.3.2. Compressive Sensing based Position Estimation

The key to apply CS ideas is to find a linear transformation, one that is able to connect position related signal parameters and sensor node measurements. Finding sparsity under a certain basis is also essential for the CS to be feasible. In the localization context, the sparse temporal properties of UWB channels or the implicit spatial sparsity of the

localization scenario or grid, where potential targets cover small part of the discrete spatial domain, could be exploited.

In the context of two-steps localization, CS doesn't necessarily need to aim to reconstruct accurately signals since the first stage of the problem is more of a parameter estimation case. The interest lies on maintaining the estimation accuracy even with a reduced number of measurements, which will result in a substantial complexity improvement in wireless networks that use UWB positioning, because of their high sampling requirements.

The CS framework has been effectively applied in communications applications such as channel estimation in ODFM [16] and UWB [27]. From the compressive measurements, the impulse response is reconstructed by l_1 minimisation methods thanks to the sparse structure of large bandwidth channels.

One of the initial works on sparsity-based indoor localization in WSN was [17], since then many approaches use different schemes of positioning and sparsity models. To name a few examples: In [18] they exploit discrete sparsity pattern in the grid location using reconstructed UWB signals from reduced volume of data in a distributed wireless sensor network. Sparsity in the spatial domain is also exploited in [19] using DPE for multi-target estimation and with a TDOA approach in [20]. All of these techniques aim to reduce the computational and storage demands to make the target localization in WSN viable.

But there has been CS applied to non-range based techniques like for example, a CS-based RSS method for indoor wireless networks [21], where the received signal strengths from a mobile tag at different WLAN Access Points (AP's) is used to create a radio map, which serves as the sparse model. CS theory is able to recover the RSS radio map with a reduced number of measurements and an improvement on the localization accuracy compared to traditional methods used in the literature.

3. Methodology / project development:

3.1. IR UWB Signal Model

The transmitted UWB signal can be written as,

$$s(t) = \sum_{j=0}^{\infty} \sum_{k=0}^{Nf-1} a_j p(t - kT_f - jT_{sym}) \quad (3.1)$$

Where the coefficient $a_j \in \pm 1$ is the j_{th} transmitted bit, T_{sym} is the symbol duration and $T_f = \frac{T_{sym}}{Nf}$ is the Pulse Repetition Period (PRF), also referred as Time of Frame. To simplify the scenario, it is assumed $a_j = 1$. Therefore, the tag is considered to periodically transmit IR-UWB pulses of very short duration.

The single pulse waveform $p(t)$ is typically a Gaussian monocycle or one of its derivatives of duration Tp.

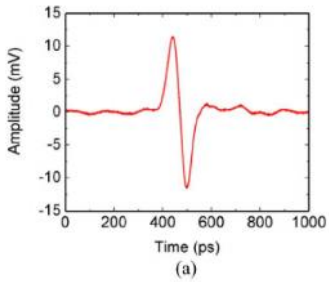

FIGURE 3.1: UWB Gaussian monocycle pulse

The signal propagates through an L-path fading channel whose response to $p(t)$ is $\sum_{l=0}^{L-1} h_l p(t - \tau_l)$ with $\tau_0 < \tau_1 < \cdots < \tau_M$, being τ_0 the delay corresponding to the LOS component. The received signal, for a given symbol, is then the summation of multiple delayed and attenuated replicas of the received pulse waveform $\tilde{p}(t)$, which includes the antenna and filters distortion. It can be expressed as:

$$y(t) = \sum_{l=0}^{L-1} \sum_{k=0}^{Nf} h_l p(t - kT_f - \tau_l) + w(t) \quad (3.2)$$

Where $w(t)$ is Additive White Gaussian Noise (AWGN) and is statistically modelled as $\mathcal{N}(0, {\sigma_w}^2)$. The signal associated to the k_{th} transmitted pulse, in the frequency domain, turns out to be:

$$Y_k(w) = h_0 S_k(w) e^{-jw\,\tau_0} + \sum_{l=0}^{L-1} h_l\, S_k(w) e^{-jw\,\tau_l} + V_k(w) \quad (3.3)$$

Where the Line-of-Sight (LOS) component is separated in the first term from the signal replicas associated to multipath. The frequency component associated to the shifted pulse is given by:

$$S_k(w) = \tilde{P}(w)e^{-j\omega kT_f} \quad (3.4)$$

Where $\tilde{P}(w)$ denotes the Fourier Transform of the pulse $\tilde{p}(t)$ and $V_k(w)$ is the noise in the frequency domain associated to the k_{th} symbol.

Sampling (3.3) at $w_m = \frac{2\pi}{N}m$ for $m = 0 \dots M-1$ and rearraging the frequency domain samples $Y_k[m]$ into the vector $\boldsymbol{y}_k \in \mathbb{C}^{Mx1}$ yields:

$$\boldsymbol{y}_k = h_0\boldsymbol{S}_k\boldsymbol{e_{\tau 0}} + \tilde{\boldsymbol{v}}_k \quad (3.5)$$

Where $\tilde{\boldsymbol{v}}_k = \boldsymbol{S}_k\boldsymbol{E}\boldsymbol{h} + \boldsymbol{v}_k$ and $\boldsymbol{S}_k \in \mathbb{C}^{MxM}$ is a diagonal matrix whose components are the frequency samples of the shifted pulse. The matrix $\boldsymbol{E} \in \mathbb{C}^{Mx(L-1)}$ contains the delay-signature vectors associated to each arriving delayed signal (multipath),

$$\boldsymbol{E} = [\, \boldsymbol{e_{\tau 1}} \;\; \dots \; \boldsymbol{e_{\tau l}} \;\; \dots \;\; \boldsymbol{e_{\tau L-1}} \,] \quad (3.6)$$

with $\boldsymbol{e_{\tau l}} = [\, 1 \;\; e^{-j\frac{2\pi}{M}\tau_l} \;\; \cdots \;\; e^{-j\frac{2\pi}{M}(M-1)\tau_l} \,]^T$. The channel fading coefficients are represented in the discrete domain too as $\boldsymbol{h} = [\, h_1 \;\cdots\; h_{L-1} \,]^T \in \mathbb{R}^{(L-1)x1}$, notice that the LOS fading contribution h_o is excluded, and the noise samples in vector $\boldsymbol{v}_k \in \mathbb{C}^{Mx1}$

3.2. CS-based Position Estimation Models

In this section, the linearized models used in this work to apply CS-positioning in UWB channels are presented.

3.2.1. CS Direct Position Estimation Model

The positioning approach that attempts to solve the problem in a single step followed by a multi-dimensional search over the spatial coordinates of the plane, with a frequency domain perspective, was proposed in [12].

The CS framework is combined with this high resolution Periodogram-based DPE approach to jointly estimate the location of the target. Firstly, the system model equation is rearranged to account for all the anchor nodes, in other words, the new observation frequency sample vector is redefined as the concatenation of signals received from all anchors:

$$\boldsymbol{y}_k = (\, \boldsymbol{y}_k{}^{(1)}, \dots, \boldsymbol{y}_k{}^{(n)}, \dots, \boldsymbol{y}_k{}^{(Na)} \,)^T$$
$$\boldsymbol{y}_k = \overline{\boldsymbol{S}}_{k,0}\boldsymbol{e_p} + \tilde{\boldsymbol{v}}_k \quad (3.7)$$

With $\bar{\boldsymbol{S}}_{k,0} = diag(h_{0,1}\boldsymbol{S}_k, \dots, h_{0,Na}\boldsymbol{S}_k)$ being a block diagonal matrix with pulse spectral components weighted by LOS channel fading coefficients, $\boldsymbol{e_p} = (\boldsymbol{e}_{f_1(\boldsymbol{p})}, \dots, \boldsymbol{e}_{f_{Na}(\boldsymbol{p})})^T$ the steering vectors as a function of the target spatial coordinates $\boldsymbol{p} = [\,x\,, y\,]^T$, and $\widetilde{\boldsymbol{v}}_k = (\widetilde{\boldsymbol{v}}_k{}^{(1)}, \dots, \widetilde{\boldsymbol{v}}_k{}^{(n)}, \dots, \widetilde{\boldsymbol{v}}_k{}^{(Na)})^T$. The steering vectors $\boldsymbol{e}_{f_n(\boldsymbol{p})}$ are defined as in (3.6), but in this case the delay is related to the position vector $\boldsymbol{p}$ by the geometrical relation $f_n(\boldsymbol{p}) = \frac{\|\boldsymbol{p}-\boldsymbol{p_n}\|}{\boldsymbol{c}}$ with $\boldsymbol{p_n}$ being the coordinates of the n_{th} anchor node.

The DPE position is given by the location vector that maximizes the following cost function,

$$\widehat{\boldsymbol{p}} = \arg\max_{\boldsymbol{p}} \boldsymbol{e_p}^{\boldsymbol{H}} \boldsymbol{R}\, \boldsymbol{e_p} \tag{3.8}$$

Where $\boldsymbol{R}$ denotes the sample covariance matrix and it is computed by averaging over properly aligned frequency samples of all anchors:

$$\boldsymbol{R} = \frac{1}{\boldsymbol{Nf}} \sum_{\boldsymbol{k=1}}^{\boldsymbol{Nf}} \boldsymbol{y}_k\ \boldsymbol{y}_k{}^H \in \mathbb{C}^{M \cdot Na\ x\ M \cdot Na} \tag{3.9}$$

Being N_f the number of observed frames used for averaging. The optimization of (3.8) can be computed by a grid search method or other stochastic methods. The cost function can be interpreted as the power-position profile because it provides the signal energy distribution with respect to spatial position.

Based on the sparsity of the target scenario, i.e., the number of unknown targets is small in the discrete spatial domain, hence the cost function or power-position profile can fit as a sparse or compressible representation.

Consider a subset of the complete local observation in an anchor node, by applying a sensing matrix:

$$\breve{\boldsymbol{y}}_k{}^{(n)} = \Phi \boldsymbol{y}_k{}^{(n)} \tag{3.10}$$

This matrix Φ is given by selecting N rows from the identity matrix $\mathbf{I}_M$, so it takes N samples of the observation vector $\boldsymbol{y}_k$ $(N < M)$, assuming a uniform distribution.

The CS-based reconstruction of the power-position profile from compressive measurements can be implemented if there is a linear model relating the random compressive measurements and the energy of the power-position profile. Assuming the target area is partitioned into a finite grid of dimensions $N_x \cdot N_y$.The following model is proposed:

$$\breve{\boldsymbol{R}} = \sum_{i=0}^{Nx\ Ny-1} \sigma_{\boldsymbol{p_i}} \breve{\boldsymbol{e}}_{\boldsymbol{p_i}} \breve{\boldsymbol{e}}_{\boldsymbol{p_i}}{}^H + \breve{\boldsymbol{R}}_{\boldsymbol{\varepsilon}} \tag{3.11}$$

Where $\breve{\boldsymbol{R}} \in \mathbb{C}^{N \cdot Na\ x\ N \cdot Na}$ is the compressed version of the sample covariance matrix, which can be computed as $\breve{\boldsymbol{R}} = \frac{1}{\boldsymbol{Nf}} \sum_{\boldsymbol{k=1}}^{\boldsymbol{Nf}} \breve{\boldsymbol{y}}_k\ \breve{\boldsymbol{y}}_k{}^H$, keeping in mind that $\breve{\boldsymbol{y}}_k$ is the concatenation of compressed signals from all anchors. $\breve{\boldsymbol{R}}_{\boldsymbol{\varepsilon}}$ represents imperfections of the model and $\sigma_{\boldsymbol{p_i}}$ is the scene energy indicator of location $\boldsymbol{p}_i$, which can be seen as the output of the cost function in (3.8). These values, $\sigma_{\boldsymbol{p_i}}$, are concatenated in a column vector of dimensions

$N_x N_y \; x \; 1$ to form $\boldsymbol{\sigma}$ .Finally, vector $\check{\boldsymbol{e}}_{\boldsymbol{p_i}} = (\Phi \boldsymbol{e}_{f_1(\boldsymbol{p_i})}, \dots, \Phi \boldsymbol{e}_{f_{Na}(\boldsymbol{p_i})})^T$ denotes the compressive steering vector corresponding to the grid location $\boldsymbol{p}_i$.

Following the sparse notation, the classic compressive sensing equation can now be written:

$$\check{\boldsymbol{r}} = \boldsymbol{A}\boldsymbol{\sigma} + \boldsymbol{r}_{\boldsymbol{\varepsilon}} \tag{3.12}$$

Where $\check{\boldsymbol{r}}$ is a $(NN_a)^2 x 1$ vector formed by the concatenation of the columns of $\breve{\boldsymbol{R}}$ .To clarify the notation, the operator $vec(\cdot)$ will be in charge of this operation, then $\check{\boldsymbol{r}} = vec(\breve{\boldsymbol{R}})$. The matrix $\boldsymbol{A}$ is the dictionary where $\boldsymbol{\sigma}$ becomes sparse and also incorporates the sensing operation. The columns of $\boldsymbol{A}$ contain the vectorised candidate covariance matrices corresponding to the different target locations $\boldsymbol{p}_i$ that conform the spatial scanning grid, the dictionary is defined as:

$$\boldsymbol{A} = [\, \check{\boldsymbol{r}}(\boldsymbol{p}_0) \; \cdots \; \check{\boldsymbol{r}}(\boldsymbol{p}_{N_x N_y - 1}) \,] \tag{3.13}$$

Where $\check{\boldsymbol{r}}(\boldsymbol{p}_i) = vec(\check{\boldsymbol{e}}_{\boldsymbol{p_i}} \check{\boldsymbol{e}}_{\boldsymbol{p_i}}{}^H)$ .The elements different from zero of $\boldsymbol{\sigma}$ represent the grid points that might indicate possible locations of targets.

The sparse vector $\boldsymbol{\sigma}$ reconstruction from the compressive measurements can be formulated as the following minimisation problem:

$$\min_{\boldsymbol{\sigma}} \|\boldsymbol{\sigma}\|_{l_1} \; subject \; to \; \check{\boldsymbol{r}} \approx \boldsymbol{A}\boldsymbol{\sigma} \tag{3.14}$$

The reconstruction algorithms used along with their performance in UWB channels are discussed in the Results section.

3.2.2. CS-Periodogram based Position Estimation Model

In this new positioning framework, we adapt the basic principles of the previous compressive sensing model, but the recovery is now carried out locally at each reference node. This change aims to exploit a different kind of sparsity and implement the positioning in a two steps fashion.

This shift in the way the sparsity is exploited is motivated due to the fact that the temporal behaviour of UWB wireless channels, in particular, the channel's impulse response, whose fading coefficients decay rapidly with time, results in a compressible structure in the delay domain. Indeed, a large portion of multipath reflections are much attenuated and the dominant reflections just become sparser.

Consider again a subset of observation vector in the frequency domain at the $n\text{-}th$ anchor node:

$$\check{\boldsymbol{y}}_k{}^{(n)} = \Phi \boldsymbol{y}_k{}^{(n)}$$

In the first stage, a linear model relating the power-delay profile or pseudo-periodogram and the random compressive measurements at each anchor node is used. Assuming the time-delay axis is divided in N_τ points. The following model, which is basically the same as (3.11) but in the delay domain, is proposed:

$$\breve{\boldsymbol{R}}_{\boldsymbol{n}} = \sum_{i=0}^{N_\tau} \sigma_{\boldsymbol{\tau_i}} \breve{\boldsymbol{e}}_{\boldsymbol{\tau_i}} \breve{\boldsymbol{e}}_{\boldsymbol{\tau_i}}^{H} + \breve{\boldsymbol{R}}_{\boldsymbol{\varepsilon}}^{(\boldsymbol{n})} \tag{3.15}$$

Where $\breve{\boldsymbol{R}}_{\boldsymbol{n}} \in \mathbb{C}^{N\,x\,N\cdot}$ is the compressed version of the sample covariance matrix, which can be computed as $\breve{\boldsymbol{R}}_{\boldsymbol{n}} = \frac{1}{Nf}\sum_{\boldsymbol{k=1}}^{Nf} \breve{\boldsymbol{y}}_k^{(\boldsymbol{n})}\, \breve{\boldsymbol{y}}_k^{(\boldsymbol{n})^H}$. $\breve{\boldsymbol{R}}_{\boldsymbol{\varepsilon}}^{(\boldsymbol{n})}$ represents imperfections of the model and $\sigma_{\boldsymbol{\tau_i}}$ is the energy indicator of delay $\boldsymbol{\tau_i}$. These values, $\sigma_{\boldsymbol{\tau_i}}$, are concatenated in a column vector of dimensions $N_\tau\, x\, 1$ to form $\boldsymbol{\sigma}$. Finally, vector $\breve{\boldsymbol{e}}_{\boldsymbol{\tau_i}} = \Phi \boldsymbol{e}_{\boldsymbol{\tau_i}}$ denotes the compressive steering vector corresponding to the delay $\boldsymbol{\tau_i}$.

Following the sparse notation, the classic compressive sensing equation can now be written:

$$\breve{\boldsymbol{r}}_{\boldsymbol{n}} = \boldsymbol{A}\boldsymbol{\sigma}_{\boldsymbol{n}} + \boldsymbol{r}_{\boldsymbol{\varepsilon}}^{(\boldsymbol{n})} \tag{3.16}$$

Where $\breve{\boldsymbol{r}}_{\boldsymbol{n}}$ is a $(N)^2 x 1$ vector formed by applying the $vec(\cdot)$ operator. The matrix $\boldsymbol{A}$ is the dictionary where $\boldsymbol{\sigma}$ becomes sparse and also incorporates the sensing operation. The columns of $\boldsymbol{A}$ contain the vectorised candidate covariance matrices corresponding to the different target locations $\boldsymbol{\tau}_i$ that conform the temporal scanning grid, the dictionary is defined as:

$$\boldsymbol{A} = [\, \breve{\boldsymbol{r}}(\boldsymbol{\tau}_0) \;\cdots\; \breve{\boldsymbol{r}}(\boldsymbol{\tau}_{N_\tau - 1}) \,] \tag{3.17}$$

Where $\breve{\boldsymbol{r}}(\boldsymbol{\tau}_i) = vec(\breve{\boldsymbol{e}}_{\boldsymbol{\tau_i}} \breve{\boldsymbol{e}}_{\boldsymbol{\tau_i}}^{H})$ .The elements different from zero of $\boldsymbol{\sigma}$ represent the grid points that might indicate possible locations of targets.

The sparse vector $\boldsymbol{\sigma_n}$ reconstruction from the compressive measurements can be formulated as the following minimisation problem:

$$\min_{\boldsymbol{\sigma_n}} \|\boldsymbol{\sigma_n}\|_{l_1} \; subject\ to\ \breve{\boldsymbol{r}}_{\boldsymbol{n}} \approx \boldsymbol{A}\boldsymbol{\sigma_n} \tag{3.18}$$

This new approach aims to make the CS recovery step anchor-wise, so another kind of sparsity can be explored. Therefore, this method can be reinterpreted as ToA-based positioning scheme.

The recovered vector $\boldsymbol{\sigma_n}$ contains the most K significant contributions of the power delay profile of the channel. The main scheme proposed to solve the second stage of the positioning model presented next.

3.2.2.1. Multi-trilateration scheme

There is a set of measures or delays estimated from each anchor that can be use in a trilateration procedure to calculate the target position. In [31], a multi-trilateration method has been developed that takes into account multiple delays $\{\tau_{l1} \cdots \tau_{lK}\}$ extracted at l-th reference node and, by using a tree-based optimization algorithm, it optimally decides the target's position by minimising a cost function .Mathematically expressed:

$$I(\boldsymbol{p}, k) = \sum_{l=1}^{Na} (\tau_l[k_l] \cdot c - \|\boldsymbol{p} - \boldsymbol{p_l}\|)^2 \tag{3.19}$$

$$\hat{\boldsymbol{p}} = \min_{\hat{\boldsymbol{p}}} I(\boldsymbol{p}, k) \tag{3.20}$$

Where $\boldsymbol{p} \in \mathbb{R}^2$ is the estimated position, $\boldsymbol{p_l} \in \mathbb{R}^2$ is the location of the l_{th} anchor node, c is the speed of light constant and $\tau_l[k_l]$, $k_l \in \{1, \dots, K\}$, are all the potential ToA's detected in the l_{th} anchor node.

The motivation to keep K paths comes from the fact that to locate the true ToA, one has to search backward from the peak location to locate any possible significant energy paths, which may not be the strongest.

The reconstruction algorithms used along with their performance in UWB channels are discussed in the Results section.

3.2.3. CS-based CIR Position Estimation Model

The last linearized model comes from the ideas derived in [29] and it is based on the theory of sparse channel estimation. The positioning scheme still resembles to the one described in the previous section in the sense that is a two steps procedure and the compressive sensing theory is applied in the first stage.

But now, the parameter estimation stage focuses on the multipath taps delays from the channel impulse response. To apply the compressive sensing framework, the sparse representation from [29] in the frequency domain is presented:

Firstly, consider the received waveform from the IR-UWB signal model in the frequency domain in (3.5) to be re-written into this form, without pointing out the LOS contribution:

$$\boldsymbol{y}_k = \boldsymbol{S}_k \boldsymbol{E} \boldsymbol{h_e} + \boldsymbol{w}_k \tag{3.21}$$

Where once again $\boldsymbol{S}_k \in \mathbb{C}^{MxM}$ is the diagonal matrix whose components are the frequency samples of the shifted pulse. The matrix $\boldsymbol{E} \in \mathbb{C}^{MxM}$ is extended to incorporate all the delay-signature vectors associated to each arriving delayed signal (multipath),

$$\boldsymbol{E} = [\, \boldsymbol{e_{\tau o}} \;\; \dots \; \boldsymbol{e_{\tau l}} \;\; \dots \;\; \boldsymbol{e_{\tau M-1}} \,] \tag{3.22}$$

With $\boldsymbol{e_{\tau l}} = [\, 1 \;\; e^{-j\frac{2\pi}{M}\tau_l} \;\; \cdots \;\; e^{-j\frac{2\pi}{M}(M-1)\tau_l} \,]^T$. The channel fading coefficients are represented in the discrete domain too as $\boldsymbol{h_e} = [\, h_1 \cdots h_{M-1} \,]^T \in \mathbb{R}^{Mx1}$ and the noise samples in vector $\boldsymbol{v}_k \in \mathbb{C}^{Mx1}$. The vector $\boldsymbol{h_e}$ can be identified as the K-sparse signal and $\boldsymbol{B} = \boldsymbol{S}_k \boldsymbol{E} \in \mathbb{C}^{MxM}$ as the dictionary where the channel becomes sparse. The noise-free version of (3.21) can be formulated as:

$$\boldsymbol{y}_k = \boldsymbol{B} \boldsymbol{h_e} = \boldsymbol{S}_k \boldsymbol{E} \boldsymbol{h_e} \tag{3.23}$$

In order to compress the frequency domain samples, a widely used random matrix $\boldsymbol{C} \in \mathbb{R}^{NxM}$ with entries i.i.d taken from a normal distribution with zero-mean and unit variance is used.

$$\breve{\boldsymbol{y}}_{\boldsymbol{k}} = \boldsymbol{C} \boldsymbol{y}_{\boldsymbol{k}} \tag{3.24}$$

Where $\breve{\boldsymbol{y}}_{\boldsymbol{k}}$ is the $Nx1$ vector of CS measurements. This illustration will help clarify the notation:

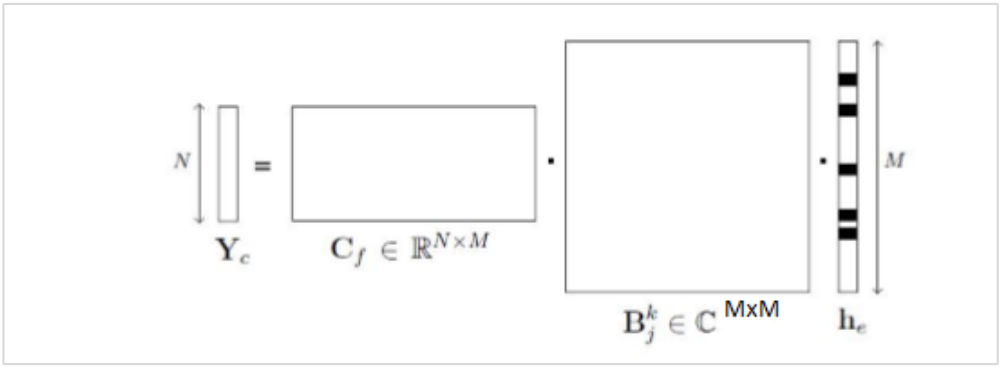

FIGURE 3.2: CS structure of channel estimation

Therefore, the sparse channel estimation $\widehat{\boldsymbol{h}}_{\boldsymbol{e}}$ can be obtained from the compressed samples $\breve{\boldsymbol{y}}_{\boldsymbol{k}}$ applying sparse signal reconstruction techniques. The sparse signal recovery problem is formulated as,

$$\min_{\boldsymbol{h_e}} \|\boldsymbol{h_e}\|_{l_1} \; subject\ to \; \boldsymbol{y}_k \approx \boldsymbol{CBh_e} \tag{3.25}$$

The estimated CIR $\widehat{\boldsymbol{h}}_{\boldsymbol{e}}$ contains the parameters of interest or, in other words, the K potential ToA's that can yield the target location through a multi-trilateration algorithm as the one described in the earlier section.

The reconstruction algorithms used along with their performance in UWB channels are discussed in the Results section.

4. Results

For the numerical evaluation of the algorithms, the channels models developed in the framework of the IEE.802.15.4a (See Appendix) are considered. In particular, the CM3 Office LOS model [28] that is characterized to exhibit dense multipath. All simulations are run with 250 independent channel realizations.

The results are given for a simplified scenario with a single target. The positioning algorithm is evaluated in 2D square setting of $6x6\ m^2$. The number of anchors has been fixed to 4, placed at each corner of the square room.

Next, in this table are summarized the parameters related to the IR-UWB signal model that remain constant throughout the simulations.

$\boldsymbol{Tp}$ (*Pulse duration*)	$1\ ns$
$\boldsymbol{Tf}$(*Time of frame*)	$56\ ns$
$\boldsymbol{Ta}$ (*Acquisition window)*	Tf
$\boldsymbol{Fs}$ **(** Sampling frequency**)**	$2\ GHz$

TABLE 4.1: Simulation Parameters

The pulse duration $\boldsymbol{Tp}$ determines the path resolution and the non-compressive sampling rate $\boldsymbol{Fs}$ translates the observation window to into $\boldsymbol{Tf} * \boldsymbol{Fs}$ samples. The sampling rates of the acquired signal $\boldsymbol{y}_k$ and, after the compression step, $\breve{\boldsymbol{y}}_k$ are related through the compression rate $\boldsymbol{\rho}$ that is defined as a follows: $= \frac{\boldsymbol{N}}{\boldsymbol{M}}$, where $\boldsymbol{M}$ represents the total number of samples acquired in a $\boldsymbol{Tf}$ window and $\boldsymbol{N}$ the total number of samples after the compression step.

The parameter $\boldsymbol{N_f}$ denotes the total number of observed data frames, to strictly focus on the behaviour of the compression, the estimator takes samples for a longer period of time as the compression rate decreases. Therefore reducing the effect of insufficient data and increasing the robustness to noise. This way the compressed observations are forced to be the same for every compression rate.

In the following table the details of the relation between these parameters are presented:

$\boldsymbol{p}$	1	0.5	0.25
$\boldsymbol{N}$	128	64	32
$\boldsymbol{N_f}$	128	256	1024

TABLE 4.2: Relationship between the parameters $\rho,\ N,\ Nf$

The metrics used to assess the localization performance simulations localization are described below:

$$RMSE(m) = \sqrt{\frac{1}{J}\sum_{j=1}^{J}\|p - \hat{p}\|^2} \qquad (4.1)$$

Where J stands for the number of channel realizations used, $p = [\,\mathrm{x}\;\;\mathrm{y}\,]^T$ is the true position of the randomly placed target in the scenario and $\hat{p} = [\,\mathrm{x}_e\;\;\mathrm{y}_e\,]^T$ is the estimated location that yield the positioning algorithms.

The estimation accuracy is determined by the root mean square error in meters. The empirical CDF (Cumulative distribution Function) of the position error is also computed in some cases for better understanding. Each point of the curves below have been generated with 250 independent channel realizations. A parametric study of the relationship between CS variables and the localization error metrics is carried out to evaluate the overall performance of the CS reconstruction algorithms.

The level of SNR is fixed to 4 dB for the assessment of the numerical performance of the algorithms. It is worth mentioning that there is signal averaging being performed in the CS-CIR model, by taking advantage of the arriving frames of one IR-UWB symbol, and the covariance matrices of the other CS models are computed over a pre-defined number of frames to improve the estimation process. Therefore, the SNR level at the end of the receiver chain is further improved with the use of these techniques.

A short review of the main CS variables is presented:

4.1. Level of Sparsity

The level of sparsity K is a requirement for the majority of standard CS algorithms, both the traditional and the model-based greedy types. For this particular application, the sparsity will be treated as a tuning parameter. Nevertheless, there are 'sparsity-aware' greedy algorithms that use different adaptive strategies to estimate the sparsity [30].

Since the sparsity is directly related to the multipath density of the UWB wireless channel, it is non obvious to select a proper value. At first sight, it may seem that a low value of sparsity should be enough to capture the paths that could yield the location.

Problems can arise if one is under-estimating or over-estimating the sparsity. If the number of paths searched, K, in the algorithm is high then there is a potential problem of picking the wrong atom (column) in the dictionary due to the noise, however, if the K, is too small then we may miss the true ToA, due to the possibility of earlier paths being weaker than the first path. Anyway, there is absolutely no interest on overfitting (high K) because the probability that the ToA path is in a far region from the LOS contribution is very low.

A large value of sparsity increases approximately the overall running time of the CS reconstruction algorithm by a factor of $O(\log(K))$.

For the model-based case, W defines the block size and C the number of active clusters that the algorithms will seek for. The total level of sparsity is defined as $W \cdot C$.The parameter W and C are critical for right performance, because now instead of searching

for the K most significant paths, the algorithms seeks for the C most significant clusters of size W.

4.2. Compression rate

The compression rate plays a fundamental role on the performance of the recovery algorithms. Testing the effect of reducing acquired samples on the localization error provides a measure of how much the sampling demands can be cut down, which is one of the problems that UWB systems are actually facing.

Ideal compressive sensing theory states that the signal under observation can be recovered with a critical number of measurements, exactly $N = O(K \cdot log\left(\frac{M}{K}\right))$ for standard recovery and $N = O(WC)$ for model based recovery.

4.3. Performance CS-DPE Model

A parametric study of the relationship between CS variables and the localization error metrics is carried out to evaluate the overall performance of the CS reconstruction algorithms.

The CS-DPE model is special in the sense that is the most different out of the other two proposed model. It is indeed exploiting another kind of sparsity pattern, the discrete 2D grid. Therefore, we summarize the list of parameters that have been used for its testing:

- $Nx = 200\,,\ Ny = 200$
- Number of iterations for OMP: 1

Notice that the number of iterations could be set equal to the number of potential targets in the scene. The OMP is the algorithm of choice for this particular model, since the strategy is to simply find the most correlated atom of the huge dictionary that discretizes the spatial grid in $\mathrm{Nx} \cdot \mathrm{Ny}$.

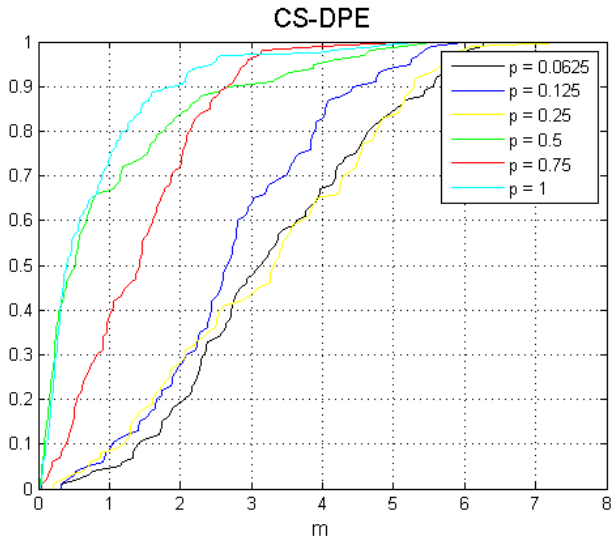

FIGURE 4.1: Rho sweep of the CDF of the error position

The CS-DPE model degrades clearly when the compression rate is low, although showing some incongruences with low values of p. OMP suits as the best CS algorithm

because its simplicity and rapid convergence, since it only requires one iteration to find the peak corresponding to the target in the spatial grid.

The huge demands of computational power and storage make the CS-DPE a very expensive technique in terms of computational resources. One key improvement will be to reduce the number of points of the grid, at the cost of increasing the gridding error.

It is well known in the literature that increasing the parameter space resolution, i.e. increasing the discrete grid where the parameter lies, tends to increase the coherence of the dictionary, which can result in to bad results.

In the next table the RMSE for each compression rate is presented:

ρ	**RMSE [m]**
0.0625	3.63
0.125	3.06
0.25	3.62
0.5	1.63
0.75	1.72
1	1.19

TABLE 4.3: RMSE as function of p for CS-DPE model

4.4. Performance CS-Periodogram Multi-ToA Model

4.4.1. Sparsity Sweep

- **Standard CS Algorithms**

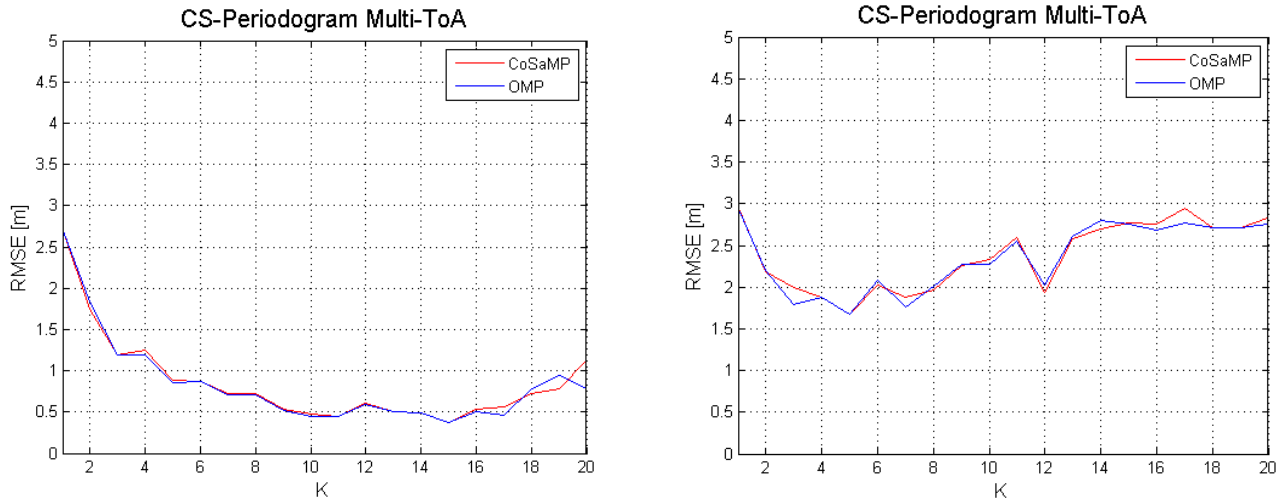

a) $p = 0.75$ b) $p = 0.25$

FIGURE 4.2: Sparsity sweep of CoSaMP and OMP

- **Block CS Algorithm**

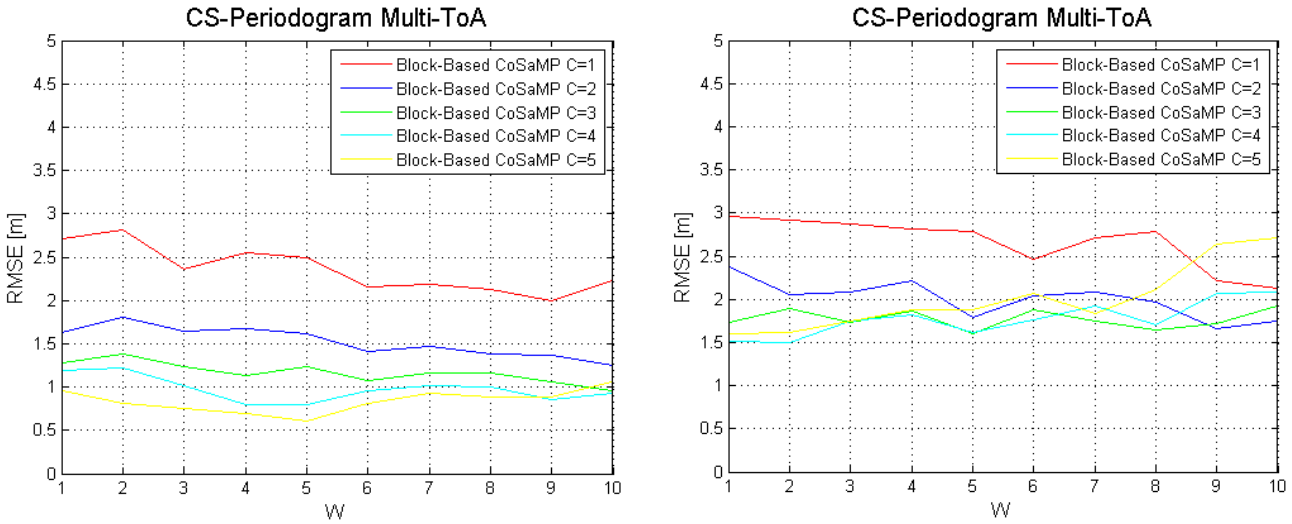

a) $p = 0.75$ b) $p = 0.25$

FIGURE 4.3: Sparsity sweep of Block-Based CoSaMP

The level of sparsity plays an important role as a tuning parameter because the number of paths to be searched for that could possibly be candidates for the true delay path is not known a priori, although it can be narrowed down to a certain range close to the strongest contribution. Both standard algorithms have very similar performance in terms of estimator accuracy, and CoSaMP's slightly better theoretical performance is not confirmed in this particular application. An interesting case for is $p = 0.25$, where quite the opposite trend that in $p = 0.75$ is going on, this due to the fact that the number of required samples to guarantee the recovery scales linearly with the level of sparsity.

In the case of model-based CS reconstruction, the block size W does not have a significant impact on the estimator's performance at any compression rate. The number of active clusters plays a far more important role , notice how when the block size is set to one sample ($W = 1$) , for any value of C, the model-based automatically corresponds to the standard CoSaMP with a level of sparsity C.

The fact that W cannot be tuned properly might be a sign that the signal under reconstruction, in this case the few clusters of the multipath arriving according to the Saleh-Valenzuela model, is not well fit under this simple structured sparsity model.

4.4.2. Compression rate Sweep

- **Standard CS algorithms**:

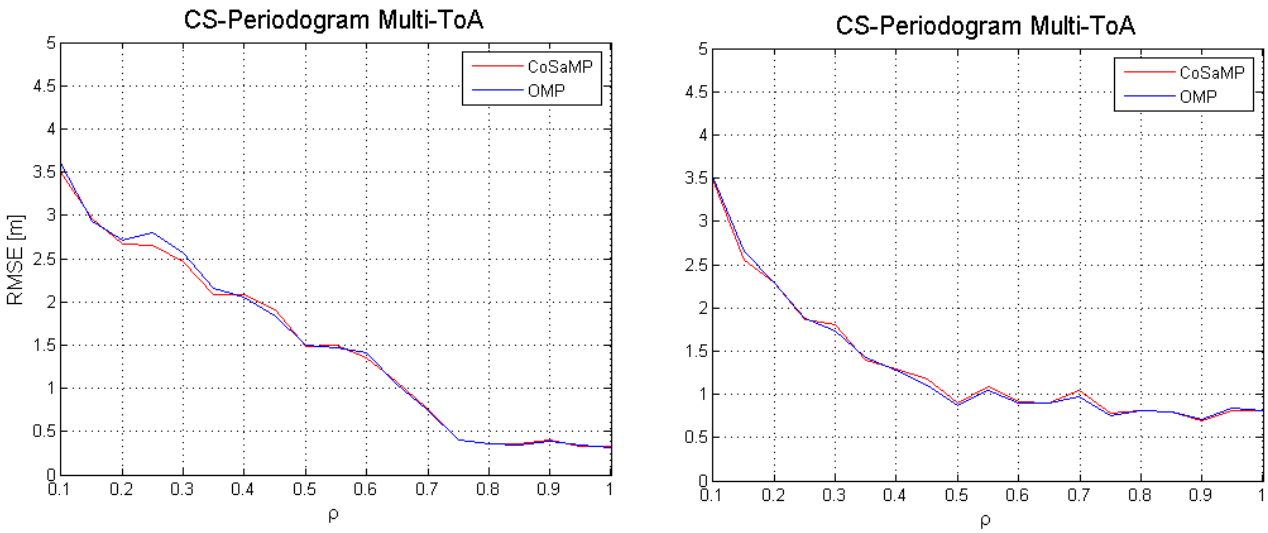

a) K=15 b) K=5

FIGURE 4.4: Compression rate sweep of CoSaMP and OMP

- **Block CS algorithm:**

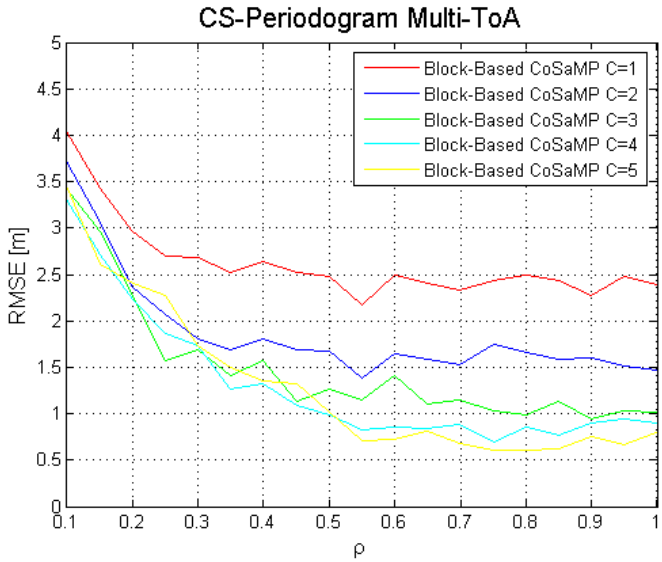

a) W=5

FIGURE 4.5: Compression rate sweep of Block-Based CoSaMP

In these graphs, it is clear that there is an expected trade-off between the compression rate chosen and the estimator's accuracy. For all levels of sparsity, the RMSE degrades

significantly as it approaches a fourth of the original sampling rate, i.e. $p = 0.25$. For a lower sparsity level, the RMSE holds a bit longer as the compression rate goes up ($\downarrow\downarrow \rho$) .

The standard CS recovery algorithms with a low level of sparsity seem to be performing almost equally to the block-based algorithm when the latter considers a medium number of active clusters ($C = 4, C = 5$), even though it is employing a larger total level of sparsity ($W \cdot C$). The more relaxed measurement bound of the model-based can be seen taking effect, since the RMSE does not degrade so quickly.

4.4.3. Signal-To-Noise Ratio Sweep

- **Standard CS Algorithms**

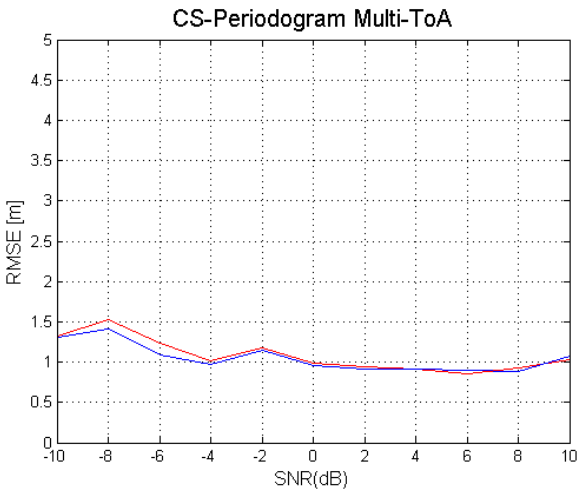

a) p=0.5 and K=10

FIGURE 4.6: SNR sweep for CoSaMP and OMP

- **Block CS algorithm**

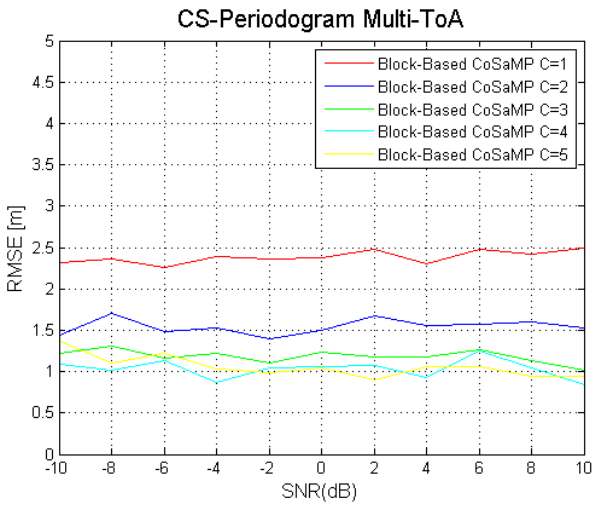

a) p =0.5 and W=5

FIGURE 4.7: SNR sweep of Block-based CoSaMP

The SNR sweep is carried out in order to see the robustness of the CS algorithms against noise. Nonetheless, the number of frames, here fixed, to compute the covariance matrix of the Position Estimation model is still kept high , meaning that for this range of level of SNR , the positioning algorithm still can perform if enough averaging is done.

4.5. Performance of CS- CIR MultiToA Model

4.5.1. Sparsity Sweep

- **Standard CS algorithms**

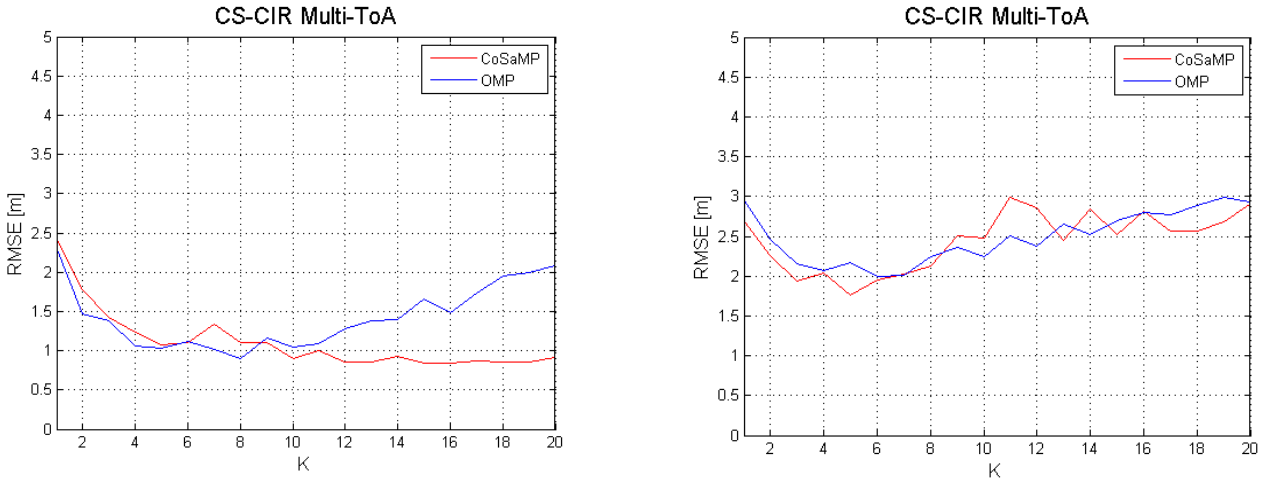

a) $p = 0.75$ b) $p = 0.25$

FIGURE 4.8: Sparsity sweep of CoSaMP and OMP

- **Block CS algorithm**

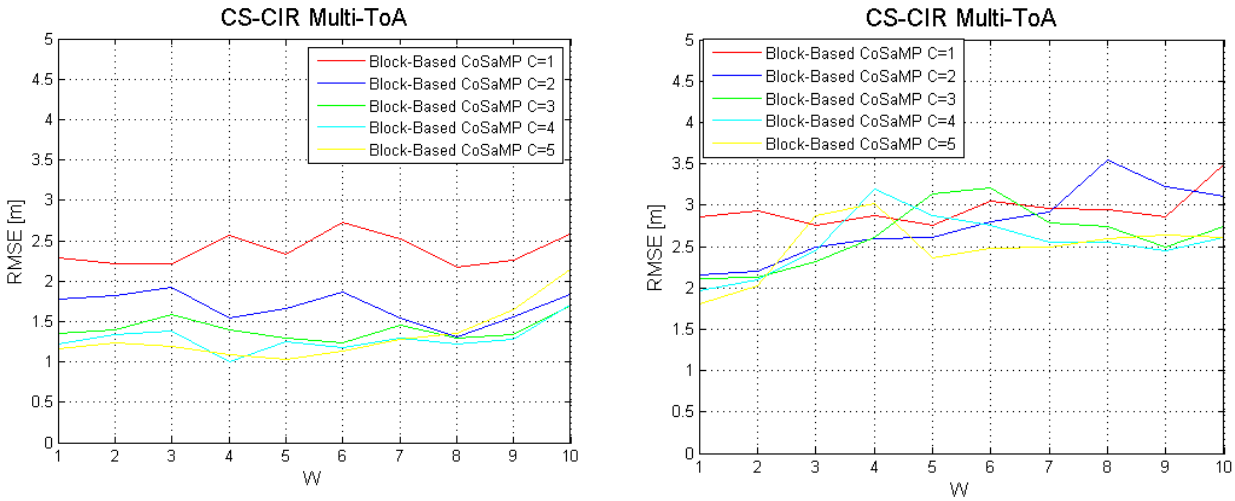

a) $p = 0.75$ b) $p = 0.25$

FIGURE 4.9: Sparsity sweep of Block-Based CoSaMP

In 4.7 a), CoSaMP has a steady decrease of the RMSE as the level of sparsity increases until it reaches a lower bound. In the other hand, OMP breaks down when a certain level is surpassed. This observation contrasts with the CS-periodogram model, where both achieve the same numerical performance. Similar effects in the tuning of this parameter are observed if compared with the anterior CS model for the family of standard algorithms. For different compression rate, the tuning seems to indicate that the optimal values of sparsity for the localization problem ought to be low.

For the block-based algorithm, the block length , once again, is not critical to the localization performance. The performance of the Block-Based CoSaMP is pretty similar in terms RMSE to the standard methods. As the number of active clusters assumption increases, the performance just gets better. One of the initial reasons of using a block-based sparsity model was to capture the LOS cluster containing the LOS path and its neighbours, but the results indicate that is not the right strategy.

4.5.2. Compression rate Sweep

- **Standard CS Algorithms:**

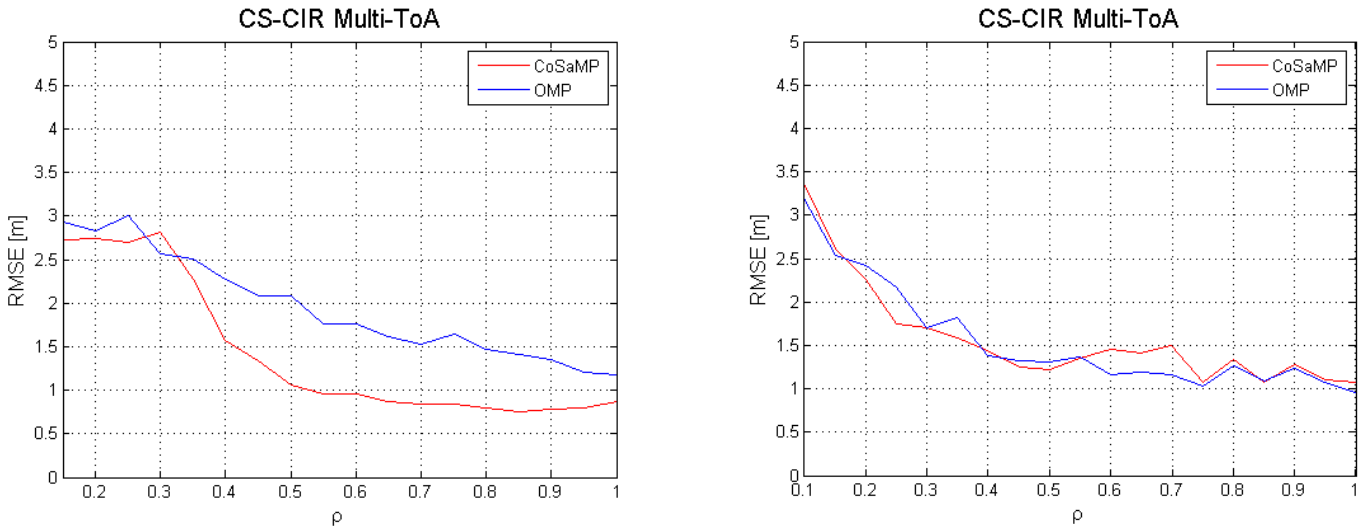

a) $K = 15$ b) $K = 5$

FIGURE 4.10: Compression rate sweep of CoSaMP and OMP

- **Block CS algorithm**:

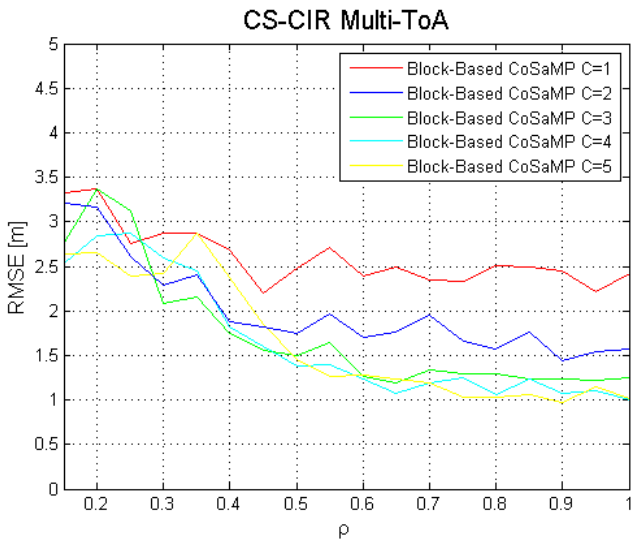

a) $W = 5$

FIGURE 4.11: Compression rate sweep of Block-based CoSaMP

The dependence of the performance error in meters on the number of measurements becomes quite clear on both, standard and block-based, algorithms.

4.5.3. Signal-to-Noise Ratio Sweep

- **Standard CS Algorithms**

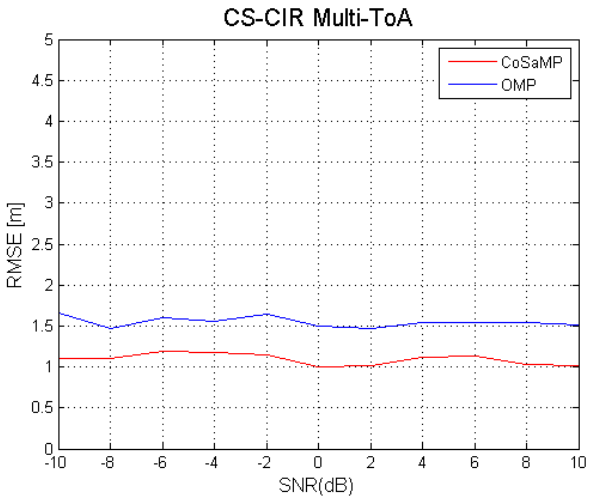

a) p=0.5 and K=10

FIGURE 4.12: SNR sweep for CoSaMP and OMP

- **Block CS algorithm**

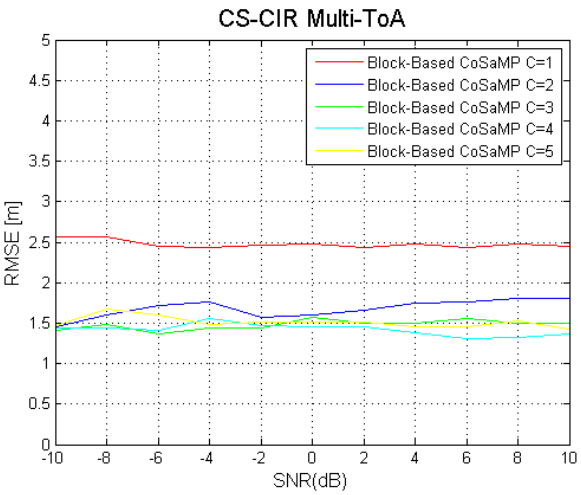

b) p =0.5 and W=5

FIGURE 4.13: SNR sweep of Block-based CoSaMP

The number of frames has been fixed for this sweep. The overall performance on this range of SNR level of all the algorithms stays constant, meaning that the signal averaging

of the different frames that it is used in the CS-CIR model to increase robustness against noise is effective. One inconvenient of the strong signal averaging is that we are penalizing high-data rate communications that could complement the IR-UWB positioning system.

4.6. Comparison

Finally, we compare the three proposed models:

- **Overall Error performance**

CS-Periodogram Multi-ToA and *CS-CIR Multi-ToA* models have very similar a performance in terms of localization error. They basically differ on the design of the CS dictionary, the *CS-Periodogram Multi-ToA* does not include the parameterized waveforms (atoms) that closely matches the information-carrying pulse shape and the *CS-CIR Multi-ToA* definitely includes the pulse contribution in its dictionary, thus leading a sparser representation of the signal to be recovered . For both models, the cluster-based reconstruction algorithm fails to outperform clearly the standard methods. Initially, it was thought that the transition from *CS-Periodogram* to the *CS-CIR* based model will help boosting the cluster-based CoSaMP performance because ,related to the previous comment on the design difference of the dictionary, the signal being recovered was now more suited to fit for the cluster model. But that was not the case. Extracting the channel statistical parameters and relating them to W, block size, and C , the number of active clusters, was another strategy applied that continued to fail.

The *CS-DPE* model seems to be outperformed by the CS based two steps strategies that employed a novel multi-trilateration. To further improve the *CS-DPE*, a finer search strategy than simply looking for the strongest correlated atom in the 2D grid space and finding a trade-off between the grid points and computational load would be necessary.

- **Running time**

The time complexity of the CS algorithms is mostly polynomial with time and they do not suppose a bottleneck in the whole process, except for the *CS-DPE* where the dictionaries can get very large and require huge amounts of storage. Anyway, the *CS-CIR* model was found to best in terms of running time, closely followed by the *CS-Periodogram* model.

5. Budget

This work is based on theoretical analysis and numerical assessment of some algorithms with the help of the Matlab software.

6. Conclusions and future development:

The novel technique of CS-based positioning presented in this Degree Thesis has still not reached its full potential. It has been proved that choice of the CS reconstruction algorithm that implements the ToA estimation stage is not a critical factor, but rather the assumption of the signal model under reconstruction, specifically, the dense multipath that UWB channels exhibit. It surely can make a difference to boost the performance.

In the lines of possible future development, there are two directions that can be taken, the first consists on modifying the current standard CS algorithms by incorporating strategies based on a few priori knowledge when selecting the most correlated atoms in the dictionary, for example, taking into account the fact that the ToA path is not far away from the strongest contribution .The second one is to find a structured sparsity based CS algorithm that adjusts better to the dynamic cluster-based model of the challenging multipath, and provides a more flexible framework in the sense that requires less demands of heuristics.

The ultimate goal would be to achieve sub-meter accuracy in situation of significant reduction of the samples acquired. The numerical assessment has proven that greatly lowering the number of measurements degrades the localization capabilities of IR-UWB systems.

CS framework provides a very interesting signal processing paradigm in the indoor UWB localization context. Even though the quality of the novel position estimation technique can still be upgraded, the foundations of the procedure have been provided and the quantitative analysis shows that it still can perform in very harsh conditions.

It has been shown that the fusion of sparse-based techniques with positioning algorithms is possible, and that the best candidate for the CM3 Office LOS channel is the CS-Periodogram position estimation model that slightly outperforms the CS-CIR position estimation model and definitely exceeds the localization performance of the CS-Direct Positioning model.

Bibliography:

[1] R. Baraniuk. Compressive sensing. IEEE Signal Processing Mag., 24(4):118–120, 124, 2007.

[2] E. Candès. Compressive sampling. In Proc. Int. Congress of Math., Madrid, Spain, Aug. 2006.

[3] E. Candès, J. Romberg, and T. Tao. Robust uncertainty principles: Exact signal reconstruction from highly incomplete frequency information. IEEE Trans. Inform. Theory, 52(2):489–509, 2006.

[4] D. Donoho. Compressed sensing. IEEE Trans. Inform. Theory, 52(4):1289–1306, 2006.

[5] E. Candès and T. Tao. Decoding by linear programming. IEEE Trans. Inform. Theory, 51(12):4203–4215, 2005

[6] E. J. Candes, J. Romberg, and T. Tao, "Stable Signal Recovery from Incomplete and Inaccurate Measurements," Communications on Pure and Applied Mathematics, vol. 59, no. 8, pp. 1207–1223, 2006.

[7] J. Tropp and D. Needell, "CoSaMP: Iterative Signal Recovery from Incomplete and Inaccurate Samples," Applied and Computational Harmonic Analysis, vol. 26, no. 3, pp. 301–321, Apr, 2008.

[8] Tropp and Gilbert, "Signal recovery from random measurements via Orthogonal Matching Pursuit," Trans. IT, Dec. 2007.

[9] "First Report and Order 02-48," tech. rep., Federal Communications Commission, Feb, 2002.

[10] IEEE Standard for Information Technology-Telecommunications and Information Exchange between Systems-Local and Metropolitan Area Networks-Specific Requirement Part 15.4: Wireless Medium Access Control (MAC) and Physical Layer (PHY) Specifications for Low-Rate Wireless Personal Area Networks (WPANs), IEEE Std 802.15.4a-2007 (Amendment to IEEE Std 802.15.4-2006), 2007, 1–203.

[11] A.J. Weiss, "Direct Position Determination of Narrowband Radio Frequency Transmitters," IEEE Signal Process. Letters, vol. 11, no. 5, pp. 513–516, May, 2004.

[12] P. Closas, C. Fernandez-Prades, and J.A. Fernandez-Rubio, "Direct Position Estimation Approach Outperforms Conventional Two-Steps Positioning," European Signal Processing Conference (EUSIPCO), Glasgow, Scotland, Aug, 2009.

[13] M.Eric and D.Vucic, "Direct Position Estimation of UWB Transmitters in Multipath Conditions," IEEE Int. Conf. Ultra-WideBand (ICUWB), Hannover, Germany, Sep, 2008.

14] M. Navarro, P. Closas, and M. Najar, "Assessment of Direct Positioning for IR-UWB in IEEE 802.15.4a Channels," IEEE Int. Conf. UltraWideBand (ICUWB), Sydney, Australia, Sep, 2013.

[15] O. Bialer, D. Raphaeli and A. J. Weiss, "Maximum-Likelihood Direct Position Estimation in Dense Multipath," in IEEE Transactions on Vehicular Technology, vol. 62, no. 5, pp. 2069-2079, Jun 2013.

[16] J. L. Paredes, G. R. Arce and Z. Wang, Ultra-Wideband Compressed Sensing: Channel Estimation, IEEE J. Select. Top. Sig. Proc., Vol. 1, no. 3, pp. 383-395, Oct 2007.

[17] D.Yang , H. Li, and G.Peterson, "Compressive Sensing Sub-mm Accuracy UWB Positioning Systems: A Space-Time Approach", Digital Signal Processing , vol 23, no. 1, pp.340-354, Jan, 2013.

[18] V. Cevher , M. F. Duarte and R. G. Baraniuk "Distributed target localization via spatial sparsity", 16th Eur. Signal Process. Conf., 2008.

[19] W. Ke and L. Wu, "Sparsity-Based Multi-Target Direct Positioning Algorithm Based on Joint-Sparse Recovery," Progress In Electromagnetics Research C, vol. 27, pp. 99–114, 2012.

[20] M. Pourhomayoun , M.Fowler and N.Wu, " Spatial Sparsity Based Emitter Localization" Conf. on Information Sciences and Systems (CISS) , Princeton, NJ,USA, March Mar, 2012.

[21] Feng, C., Au, W. S. A., Valaee, S., & Tan, Z. (2012). Received-signal-strength-based indoor positioning using compressive sensing. Mobile Computing, IEEE Transactions on, 11(12), 1983-1993.

[22] Lei Yu, Hong Sun, Jean-Pierre Barbot, Gang Zheng. Bayesian Compressive Sensing for Cluster Structured Sparse Signals. Signal Processing, Elsevier, 2012, 92 (1), pp.259-269.

[23] L. Yu, H. Sun, J. P. Barbot, and G. Zheng, "Bayesian compressive sensing for cluster structured sparse signals," Signal Processing (submitted), 2010.

[24] Y. C. Eldar, P. Kuppinger, and H. Bolcskei, "Block-sparse signals: Uncertainty relations and efficient recovery," IEEE Trans. Signal Process., vol. 58, no. 6, pp. 3042–3054, 2010

[25] V. Cevher, P. Indyk, C. Hegde, and R. G. Baraniuk, "Recovery of clustered sparse signals from compressive measurements," in Int. Conf. on Sampling Theory and Applications (SAMPTA), 2009.

[26] R. G. Baraniuk, V. Cevher, M. F. Duarte and C. Hegde, "Model-Based Compressive Sensing," in IEEE Transactions on Information Theory, vol. 56, no. 4, pp. 1982-2001, April 2010.

[27] J. L. Paredes, G. R. Arce and Z. Wang, "Ultra-Wideband Compressed Sensing: Channel Estimation," in IEEE Journal of Selected Topics in Signal Processing, vol. 1, no. 3, pp. 383-395, Oct. 2007.

[28] Molisch, A. F. (2004). IEEE802. 15.4 a Channel model subgroup final report.IEEE P802, 15, 943-968.

[29] E. Lagunas and M. Nájar, "Sparse channel estimation based on compressed sensing for ultra-wideband systems," Ultra-Wideband (ICUWB), 2011 IEEE International Conference on, Bologna, 2011, pp. 365-369.

[30] Do, T. T., Gan, L., Nguyen, N., & Tran, T. D. (2008). Sparsity adaptive matching pursuit algorithm for practical compressed sensing. JOHNS HOPKINS UNIV BALTIMORE MD DEPT OF ELECTRICAL AND COMPUTER ENGINEERING.

[31] Genís Floriach "Position Estimation for IR-UWB Systems using Compressive Sensing" Degree Thesis, Department of Signal Theory and Communications, Universitat Politècnica de Catalunya , Barcelona, Spain.

Appendices:

CoSaMP

CoSaMP($\boldsymbol{\Phi}$, $\boldsymbol{u}$, s)
Input: Sampling matrix $\boldsymbol{\Phi}$, noisy sample vector $\boldsymbol{u}$, sparsity level s
Output: An s-sparse approximation $\boldsymbol{a}$ of the target signal

$\boldsymbol{a}^0 \leftarrow \mathbf{0}$ { Trivial initial approximation }
$\boldsymbol{v} \leftarrow \boldsymbol{u}$ { Current samples = input samples }
$k \leftarrow 0$

repeat
$k \leftarrow k + 1$

$\boldsymbol{y} \leftarrow \boldsymbol{\Phi}^* \boldsymbol{v}$ { Form signal proxy }
$\Omega \leftarrow \text{supp}(\boldsymbol{y}_{2s})$ { Identify large components }
$T \leftarrow \Omega \cup \text{supp}(\boldsymbol{a}^{k-1})$ { Merge supports }

$\boldsymbol{b}|_T \leftarrow \boldsymbol{\Phi}_T^{\dagger} \boldsymbol{u}$ { Signal estimation by least-squares }
$\boldsymbol{b}|_{T^c} \leftarrow \mathbf{0}$

$\boldsymbol{a}^k \leftarrow \boldsymbol{b}_s$ { Prune to obtain next approximation }
$\boldsymbol{v} \leftarrow \boldsymbol{u} - \boldsymbol{\Phi} \boldsymbol{a}^k$ { Update current samples }

until halting criterion *true*

Block-Based CoSaMP

Algorithm 1 Model-based CoSaMP
Inputs: CS matrix Φ, measurements y, model $\mathcal{M}_K$
Output: K-sparse approximation $\widehat{x}$ to true signal x
$\widehat{x}_0 = 0$, $r = y$, $i = 0$ {initialize}
while halting criterion false **do**
$i \leftarrow i + 1$
$e \leftarrow \Phi^T r$ {form signal residual estimate}
$\Omega \leftarrow \text{supp}(\mathbb{M}_2(e, K))$ {prune signal residual estimate according to signal model}
$T \leftarrow \Omega \cup \text{supp}(\widehat{x}_{i-1})$ {merge supports}
$b|_T \leftarrow \Phi_T^{\dagger} y$, $b|_{T^C} \leftarrow 0$ {form signal estimate}
$\widehat{x}_i \leftarrow \mathbb{M}(b, K)$ {prune signal estimate according to signal model}
$r \leftarrow y - \Phi \widehat{x}_i$ {update measurement residual}
end while
return $\widehat{x} \leftarrow \widehat{x}_i$

OMP

Algorithm Orthogonal Matching Pursuit

Input:

- A measurement matrix $\Phi \in \mathbb{R}^{m \times n}$.
- Observation vector $\mathbf{y} \in \mathbb{R}^m$.
- Sparsity level k of the ideal signal $\mathbf{x} \in \mathbb{R}^n$.

Output:

- An estimate $\hat{\mathbf{x}} \in \mathbb{R}^n$ of the ideal signal $\mathbf{x}$.
- A set Λ_k containing the positions of the non-zero elements of $\hat{\mathbf{x}}$.
- An approximation to the measurements $\mathbf{y}$ by $\mathbf{a}_k$.
- The residual $\mathbf{r} = \mathbf{y} - \mathbf{a}_k$.

1: $\mathbf{r}^{(0)} \leftarrow \mathbf{y}$ ▷ Initialise the residual
2: $\Lambda^{(0)} \leftarrow \emptyset$ ▷ Initialise the indices
3: **for** $i = 1, \ldots, k$ **do**
4: $\lambda^{(i)} \leftarrow \arg\max_{j=1,\ldots,n} \left| \left\langle \mathbf{r}^{(i-1)}, \phi_j \right\rangle \right|$ ▷ The column of Φ that is most correlated with $\mathbf{r}_{i-1}$
5: $\Lambda^{(i)} \leftarrow \Lambda^{(i-1)} \cup \lambda^{(i)}$
6: $\Phi^{(i)} \leftarrow \left[\Phi^{(i-1)} \; \phi_{\lambda^{(i)}} \right]$
7: $\mathbf{x}^{(i)} \leftarrow \arg\min_{\hat{\mathbf{x}}} \left\| \mathbf{y} - \Phi^{(i)} \hat{\mathbf{x}} \right\|_2$ ▷ Solve the Least Squares for new signal estimate
8: $\mathbf{a}^{(i)} \leftarrow \Phi^{(i)} \mathbf{x}^{(i)}$ ▷ New data approximation
9: $\mathbf{r}^{(i)} \leftarrow \mathbf{y} - \mathbf{a}^{(i)}$ ▷ New residual
10: **end for**
11: $\hat{\mathbf{x}} \leftarrow \mathbf{x}^{(k)}$
12: **return** $\hat{\mathbf{x}}, \Lambda^{(k)}, \mathbf{a}^{(k)}, \mathbf{r}^{(k)}$

IEE 802.15.14.a Channels Model

The generic channel model that is used for the 2-10 GHz model. The key features of the model are summarized:

- d^{-n} law for the path-loss
- frequency dependence of the path-loss
- modified *Saleh-Valenzuela* model:
  - Arrival of paths in clusters.
  - Mixed Poisson distribution for ray arrival times.
  - Possible delay dependence of cluster decay times.
  - Some NLOS environments have first increase, then decrease of power delay profile.
- Nakagami-distribution of small-scale fading, with different m-factors for different components
- Block fading: channel stays constant over data burst duration.

The CM3 Office model is an indoor office environment, the rooms are comparable to the size of residential homes, but some rooms (especially cubicle areas, laboratories, etc.) are considerably larger. Areas with many small offices are typically linked by long corridors. Each of the offices typically contains furniture, book shelves on the walls, etc., which adds to the attenuation given by the (typically thin) office partitionings. This model was developed under measurements covering a range of 3-28 meters and from 2-8 GHz.

List of the main parameters for the model:

- n path-loss exponent
- σ shadowing standard deviation
- PL_o path-loss at 1m distance
- A_{ant} antenna loss
- k frequency dependence

- $\bar{L}$ mean number of clusters
- Λ inter-cluster arrival rate
- λ_1 , λ_2 , β ray arrival rates (Poisson Model)
- Γ inter-cluster decay constant
- k_γ, γ_o inter-cluster decay time constants
- $\sigma_{cluster}$ cluster shadowing variance

	Office
	LOS
Pathloss	
n	1.63
σ_S	1.9
PL_0 [dB]	35.4
A_{ant}	3 dB
κ	0.03
Power delay profile	
$\bar{L}$	5.4
Λ [1/ns]	0.016
λ_1, λ_2 [1/ns], β	0.19, 2.97, 0.0184
Γ [ns]	14.6
k_γ	0
γ_0 [ns]	6.4
$\sigma_{cluster}$ [dB]	

This model is a statistical model whose basic assumption is that multipath components (MPCs) arrive in clusters, formed by the multiple reflections from the objects in the vicinity of receiver and transmitter. The clusters, as well as the MPCs within a cluster, arrive according to Poisson processes with different rates and have inter-arrival times that are exponentially distributed. The MPCs amplitudes are independent Rayleigh random variables, and the corresponding phase angles are independent uniform random variables over $(0,2\pi)$. The power decays exponentially with cluster decay as well as excess delay within a cluster.

A typical Channel Impulse Response (CIR):